LAPPEENRANTA UNIVERSITY OF TECHNOLOGY
Faculty of Technology Management
Degree Programme in Information Technology

STATISTICAL ANALYSIS AND NUMERICS OF HEAT EXCHANGER MODELS

The examiners of the thesis were Professor Heikki Haario and PhD Tuomo Kauranne.
The thesis was supervised by Professor Heikki Haario.

September 28, 2009
Taavi Aalto

ABSTRACT

Lappeenranta University of Technology
Faculty of Technology Management
Department of Information Technology

Taavi Aalto

Statistical Analysis and Numerics of Heat Exchanger Models

Thesis for the Degree of Master of Science in Technology

2009

69 pages, 26 figures, 7 tables and 1 appendix

Examiners: Professor Heikki Haario
PhD Tuomo Kauranne

Keywords: Heat exchangers, MCMC

The identifiability of the parameters of a heat exchanger model without phase change was studied in this Master's thesis using synthetically made data. A fast, two-step Markov chain Monte Carlo method (MCMC) was tested with a couple of case studies and a heat exchanger model. The two-step MCMC-method worked well and decreased the computation time compared to the traditional MCMC-method.

The effect of measurement accuracy of certain control variables to the identifiability of parameters was also studied. The accuracy used did not seem to have a remarkable effect to the identifiability of parameters.

The use of the posterior distribution of parameters in different heat exchanger geometries was studied. It would be computationally most efficient to use the same posterior distribution among different geometries in the optimisation of heat exchanger networks. According to the results, this was possible in the case when the frontal surface areas were the same among different geometries. In the other cases the same posterior distribution can be used for optimisation too, but that will give a wider predictive distribution as a result.

For condensing surface heat exchangers the numerical stability of the simulation model was studied. As a result, a stable algorithm was developed.

TIIVISTELMÄ

Lappeenrannan teknillinen yliopisto
Teknistaloudellinen tiedekunta
Tietotekniikan osasto

Taavi Aalto

Lämmönvaihdinyhtälöiden tilastollinen analyysi ja numeriikka

Diplomityö

2009

69 sivua, 26 kuvaa, 7 taulukkoa ja 1 liite

Tarkastajat: Professori Heikki Haario
FT Tuomo Kauranne

Hakusanat: Lämmönvaihdin, MCMC
Keywords: Heat exchangers, MCMC

Tässä diplomityössä tutkittiin lauhduttamattoman lämmönvaihtimen mallin parametrien määräytymistä synteetttisesti luodulla aineistolla. Parametrien posteriorijakauman selvittäminen tunnetusta aineistosta on inversio-ongelma, joka ratkaistiin Bayesin kaavan avulla. Työssä testattiin nopeaa kaksivaiheista Markov chain Monte Carlo -menetelmää (MCMC) ensin muutamalla testiesimerkillä ja sitten lämmönvaihdinyhtälöllä. Epäsuora kaksivaiheinen menetelmä osoittautui toimivaksi ja nopeutti laskentaa perinteiseen suoraan MCMC-menetelmään verrattuna.

Lisäksi tässä työssä tutkittiin kontrollimuuttujien mittausepätarkkuuden vaikutusta mallin parametrien määräytymiseen. Kontrollimuuttujien kohtuullisella mittausepätarkkuudella ei näyttänyt olevan havaittavaa vaikutusta mallin parametrien määräytymiseen.

Tässä työssä tutkittiin myös saman posteriorijakauman käyttökelpoisuutta erilaisilla lämmönvaihtimilla. Saman posteriorijakauman käyttö eri lämmönvaihtimilla olisi laskennan kannalta edullista yritettäessä optimoida lämmönvaihtimista muodostuvaa verkostoa. Saatujen tulosten mukaan samaa posteriorijakaumaa voidaan käyttää eri lämmönvaihdinten ennustejakauman laskemiseen sellaisenaan, kun lämmönvaihdinten otsapinta-ala on sama. Muutoin saatu ennustejakauma on leveämpi kuin oikealla posteriorijakaumalla laskettu ennustejakauma olisi.

Lauhduttavan lämmönvaihtimen osalta tutkittiin mallin numeriikkaa. Malli saatiin toimimaan stabiilisti ja sitä voitiin käyttää toisessa diplomityössä.

PREFACE

This research was funded by TM Systems Finland Oy for six months, as a part of a Finnish national programme on modelling and simulation (MASI), launched by Tekes.

My supervisor, professor Heikki Haario, suggested the use of indirect two step method and the use of the uncertainty in the measurement of the control variables. I thank him for proof-reading my thesis and for the hints about the indirect method.

I thank Kalle Riihimäki from Balance Engineering for proof-reading my thesis and teaching me the most essential things about heat exchangers.

I thank Tuomo Kauranne for proof-reading my thesis.

In this project I worked with Dominique Habimana from Rwanda. I thank him for our conversations about the differences in our cultures and about getting an international experience without having to leave my own country. It was an instructive experience and I even learned to understand my own culture better.

Finally I thank my wife Maarit for correcting my English. I want to apologise her and our sons, Eetu, Pekka and Olli for the long studying and research period and the time away from my family during that. Thank you for standing that.

Taavi Aalto
Lappeenranta
September 28, 2009

CONTENTS

1 INTRODUCTION **7**

2 HEAT EXCHANGERS **8**

2.1 Fundamentals of heat transfer 10

2.2 Heat transfer through a wall 11

2.3 Model of the heat exchanger without phase change 13

2.4 Model of the condensing surface heat exchanger 17

3 MODEL VARIABLES **25**

3.1 Measured variables 25

3.1.1 Measuring and measurement inaccuracy 26

3.2 Calculated variables 30

3.2.1 Mass flow 31

3.2.2 Moisture content of the air 33

3.2.3 Material properties 34

3.3 General form of a model 35

4 INVERSE PROBLEMS AND THE BAYESIAN INFERENCE **37**

4.1 The Metropolis–Hastings algorithm 38

4.2 Indirect method for MCMC 39

5 TESTS FOR THE TWO-STEP INDIRECT METHOD 42

5.1 Case study 1: Linear plane 42

5.2 Case study 2: Slope of line 43

5.3 Case study 3: Arrhenius law 44

6 STATISTICAL ANALYSIS OF THE MODEL WITHOUT PHASE CHANGE 47

6.1 Comparison of the direct and indirect methods 47

6.2 Effect of measurement sample size, design of experiments and error variance 50

6.3 Usability of the same posterior distribution among different geometries . 55

6.4 Error in measured variables 57

7 NUMERICS OF THE CONDENSING SURFACE MODEL 61

7.1 Effect of the initial guess 62

7.2 Retrial of the solution in the case of the fail of the convergence 64

7.3 Effect of the number of cells 64

8 CONCLUSIONS 66

REFERENCES 68

APPENDICES

NOTATIONS

A	pre-exponential factor in Arrhenius law	[mol/dm^{3}s]
A	heat surface area	[m^2]
A_{duct}	area of the cross-section of the duct	[m^2]
A_{slots}	frontal surface area	[m^2]
c_p	specific heat capacity	[J/kgK]
C	constant of Nusselt number (parameter)	[-]
d_{hydr}	case specific hydraulic diameter	[m]
E	activation energy in Arrhenius law	[J/mol]
f	model function	[-]
$\tilde{f}$	partial model function	[-]
F	correction factor for the cross-flow heat exchanger	[-]
g	observation function	[-]
G	set of geometry variables	[-]
h	specific enthalpy of the moist air	[J/kg]
k	correction factor for the flow rate	[-]
k	rate constant of the reaction	[mol/dm^{3}s]
k	thermal conductivity	[W/mK]
k_{wall}	thermal conductivity of the wall	[W/mK]
l	height of the slot or length of the plate	[m]
m	constant of Nusselt number (parameter)	[-]
m	mass	[kg]
M	molar mass	[kg/mol]
n	number of moles	[mol]
n	constant of Nusselt number (parameter)	[-]
n_{pass}	number of passes in combined heat exchanger unit	[-]
N_{slots}	number of cold slots in heat exchanger	[-]
Nu	Nusselt number	[-]
p	pressure	[Pa]
p_{atm}	atmospheric pressure	[Pa]
p_{bar}	pressure in bars	[bar]
p_{d}	dynamic pressure	[Pa]
p_{s}	static pressure	[Pa]
p_{sat}	saturation pressure of water vapour	[Pa]
p_{tot}	total pressure	[Pa]
Δp	pressure difference between inside and outside of the duct	[Pa]

$p(\theta)$	prior distribution	[-]
$p(\theta\|y)$	posterior distribution (also the notation $\pi(\theta)$ is used)	[-]
$p(y)$	normalising factor	[-]
$p(y\|\theta)$	likelihood density function	[-]
Pr	Prandlt number	[-]
q_m	mass flow	[kg/s]
q_V	volume flow	[m^3/s]
Q	energy	[J]
r_0	heat of vaporisation at 0 °C	[J/kg]
R	ideal gas constant	[J/Kmol]
R_h	heat capacity flow ratio	[-]
Re	Reynold's number	[-]
s	vector of the state variables	[-]
s_wall	thickness of the wall	[m]
t	time	[s]
T	temperature	[°C] / [K]
T_C	temperature in Celsius degrees	[°C]
T_dew	dew point of the moist air	[°C]
T_dry	dry bulk temperature	[°C]
T_K	temperature in Kelvins	[K]
T_wet	wet bulk temperature	[°C]
ΔT_∞	temperature difference between the hot and the cold mixed layers	[°C]
ΔT_lm	logarithmic mean temperature difference between the hot and the cold side	[°C]
U	overall heat transfer coefficient	[W/m^2K]
v	velocity	[m/s]
V	volume	[m^3]
w	width of the slot	[m]
x	vector of the control variables	[-]
x	mass fraction	[-]
$\tilde{x}$	set of model variables	[-]
$\tilde{x}$	molar fraction	[-]
x_wall	thickness coordinate of the wall	[m]
y	vector of observations	[-]
Z_h	number of transfer units	[-]

Greek alphabet

α	convective heat transfer coefficient	[W/m^{2}K]
α_{k}	overall heat transfers coefficient from the condensate to the cold flow	[W/m^{2}K]
α_{w}	convective heat transfer coefficient of condensate (water)	[W/m^{2}K]
α_{cond}	convective heat transfer coefficient during a simultaneous mass transfer	[W/m^{2}K]
β_{i}	regression coefficients	[-]
ϵ	noise vector or the error vector of observations	[-]
θ	vector of the unknown model parameters	[-]
$\tilde{\theta}$	vector of "pseudo" parameters	[-]
$\hat{\theta}$	parameter estimate	[-]
Θ	theta-function	[°C]
Θ_h	Θ-function of enthalpy	[°C]
Θ_ω	Θ-function of moisture content	[°C]
μ	dynamic viscosity of the the fluid	[Ns/m^2]
ξ	auxiliary variable in the calculation of F	[-]
$\tilde{\xi}$	auxiliary variable in the calculation of $F_{\mathrm{n_{pass}}}$ in one pass	[-]
ρ	density	[kg/m3]
σ	standard deviation (of measurement error)	[-]
ϕ	interaction term of the compounds	[-]
Φ	heat rate	[W]
Φ''	heat flux	[W/m^2]
ω	moisture content of the air	[kg/kg]
ω_{cond}	moisture content of saturated air	[kg/kg]

Indexes

a	incoming cell boundary according to hot flow
b	outgoing cell boundary according to hot flow
c	cold, value of the property on cold side
cond	condense
da	dry air
duct	duct, in the (ventilation) duct
h	hot, value of the property on hot side
he	heat exchanger, in heat exchanger

i	inlet, incoming, value of the property in the inlet
ma	moist air
o	outlet, outgoing, value of the property in the outlet
surf	surface, at the surface
w	water
wall	wall, in the wall
wv	water vapour
∞	at infinity, in mixed layer

Abbreviations

MCMC	Markov chain Monte Carlo
SS	Sum of Squares
std	standard deviation

1 Introduction

Heat exchangers are widely used in paper mills for heat recovery to decrease the costs of paper making. In paper mills different kinds of heat exchangers can be coupled together in many ways so that they produce a network of heat exchangers. It can be optimised to produce maximal heat recovery by minimal costs. If the reliability of the optimisation result is the aim of the study, some statistical analysis has to be done. This has to be started by studying the unit processes. The effects of accuracy of material property modelling on heat flow has been studied earlier by Liikola [1]. His work concentrated on traditional sensitivity analysis and even some Bayesian analysis was done. Markov chain Monte Carlo (MCMC) methods are a very efficient way to study the distributions of all model parameters, compared to traditional sensitivity analysis.

The scope of this study will be one heat exchanger unit. It will be modelled mathematically, the parameter estimation will be done by MCMC methods. Models will be "traditional" phenomenological engineering models rather than more detailed FEM-models. The posterior distribution of the parameters in heat exchanger model is estimated. Solving the model is numerically slow, so some methods to decrease the computation times are needed and these will be tested here. Measurements needed in statistical analysis are very difficult to get in our case. For that reason synthetically made data is used in analysis. Sampling will be studied from the point of view of the measurement sample size and the size of error in response.

The optimisation of a network of heat exchangers can be done, for example, by changing the geometries and the number of heat exchanger units in the network. If the results of the optimisation are to be statistically estimated, the posterior distributions of model parameters can be used in optimisation. It will be studied whether the posterior distribution of model parameters generated with one geometry can be used with another geometry, because that would be computationally the lightest way.

There is an error in the measurement of control variables — actually the case with all measurements and models. Combining units together will increase this error if measurements are not taken between units but measurements are based on the calculated values from previous unit and the measurement error there. The effect of an error in control variables to posterior distribution will be studied. Finally the numerics of the condensing heat exchanger model will be improved.

2 Heat Exchangers

Large heat exchangers are used in industry for heat recovery to save primary energy used in the process. Small heat exchangers are used at homes as radiators or in ventilation. Applications considered here are typical for paper machine dryer section air systems.

A heat exchanger is an apparatus which transfers energy from hot flow to cold flow. Flows can be separated, for example, by a tube or a plate. Fluids used in the thesis are air and water. There is always some water vapour in the air. Thus air is called moist air. Fluids can change phase inside the heat exchanger. Here it would mean that water vapour might condensate or water might evaporate. Evaporating heat exchangers are not used is conventional heat recovery systems in paper machine dryer section. For that reason phase change means hereafter always condensation, not evaporation.

If no phase change happens inside the heat exchanger — condensation of the fluid — the heat exchanger is called hereafter *noncondensing heat exchanger* or *heat exchanger without phase change*. If the phase change — condensation of the water vapour — happens inside the heat exchanger, the heat exchanger is called hereafter *condensing surface heat exchanger* or *heat exchanger with phase change*. If fluids on the both side are water, then the heat exchanger is noncondensing. Such a case will not be considered here, but the flows will be moist air in the both sides or moist air in the hot side side and water in the cold side.

Flows can be parallel, counter-current or crossing ones and the heat exchangers are called parallel-flow, counter-flow and cross-flow heat exchanger, respectively. The cross-flow plate heat exchanger will be modelled, because for practical reasons the cross-flow is most often the only possibility in paper mills. An illustration of a cross-flow heat exchanger is represented in Figure 1.

The geometry of the heat exchanger G_{he} is thought from the point of view of the particle in the fluid, where the coordinate system is Lagrangian (moving rather than static). The width of the slot between the plates is small compared to the length of the sides of the plate. For this reason the distance between the plates w is called the width of the slot and the measure along the side of the plate l is called the height of the slot. Similarly, the side of the plate perpendicular to flow is always called the height of the plate on both the hot and the cold side. Thus the information about the side of the flow has to be always given when the term height of the plate is used. A hot slot on both ends of the heat exchanger

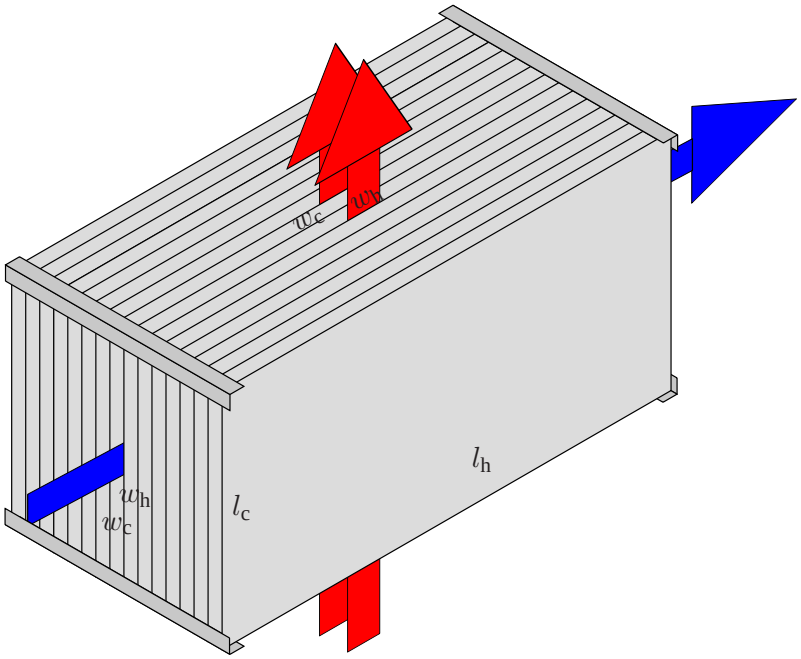

Figure 1: An illustration of a cross-flow plate heat exchanger.

is assumed. For that reason the total surface area of a heat exchanger A is two times the amount of cold slots N_{slots} multiplied by the area of one plate.

Characteristic measure or hydraulic diameter d_{hydr} is four times the area of cross section of one slot divided by the circumference of the cross section of the slot. So for a tube it is the diameter of the tube and for a plate heat exchanger it is obtained by

$$d_{\text{hydr}} = \frac{4wl}{2(w+l)} \tag{1}$$

and is about two times the width of the slot between the plates because usually the height of the slot is much more than the width of the slot. The cross-sectional area of the slots in a heat exchanger on the hot or the cold side is also called a frontal surface, A_{slots}.

A fluid is coming to the heat exchanger and passing it along a duct or a pipe. The geometry of the duct G_{duct} includes the cross-sectional area of the duct A_{duct}. It is calculated as a product of the lengths of the sides in a square duct and for a round duct by circumference measure.

In the following subsections the model without phase change and the model where condensation happens on the surface are described starting from the basics of heat transfer. More information about this topic can be found, for example, in [2] or [3].

2.1 Fundamentals of heat transfer

The conservation of energy is the first law of thermodynamics. It is used later in section 2.3. According to the second law of thermodynamics entropy is increasing. It is a reason for the phenomena that heat always transfers from hot to cold. There are three mechanisms of heat transfer: conduction, convection and radiation. In this study the radiation can be neglected because in process temperatures the effect of the radiation is not remarkable.

Conduction happens inside a material. It is caused by thermal random movement of molecules and atoms (diffusion). According to the Fourier's law heat flux Φ'' is proportional to temperature gradient. The Fourier's law in one dimensional form for a wall made of homogeneous material is

$$\Phi''_{\text{wall}} = -k_{\text{wall}} \frac{\mathrm{d}T}{\mathrm{d}x_{\text{wall}}}, \tag{2}$$

where

Φ''_{wall}	is the perpendicular heat flux of the wall inside the wall	[W/m^2],
k_{wall}	is the thermal conductivity of the wall	[W/mK],
T	is the temperature	[°C] / [K],
x_{wall}	is the thickness coordinate of the wall	[m].

Convection combines microscopic diffusion and macroscopic motion of the fluid where energy is transferred by the flow of the fluid [2, p. 6]. Heat transfer from a fluid to a solid material or the other way around is also called convection. Free convection always exists if the surface temperature of a solid material is different from the temperature of the fluid. It can be enforced by external means (enforced convection). Hereafter enforced convection is assumed because that is more efficient and used mechanism in process heat exchangers. When the fluid is enforced to flow along a surface, the velocity is zero at the surface and it increases when we go further from the surface. The layer starting from the surface and ending at the mixed layer where no change in the velocity happens anymore is called velocity boundary layer. When the temperatures of the fluid and surface of the solid material are not the same, there will be a thermal boundary layer near the surface. The temperature in the fluid near the surface is the same as on the surface. In the boundary layer the temperature will increase or decrease gradually until it reaches the temperature of the mixed layer. Convection happens from hot surface to cold fluid in the boundary

layer according to the Newton's law of cooling

$$\Phi'' = \alpha(T_{\text{surf}} - T_{\infty}), \tag{3}$$

where

Φ''	is the heat flux	[W/m^2],
α	is the convective heat transfer coefficient	[W/m^{2}K],
T_{surf}	is the temperature at the wall surface	[°C],
T_{∞}	is the temperature in the mixed layer	[°C].

2.2 Heat transfer through a wall

In heat transfer through a wall from fluid to fluid convection happens on the both sides of the wall and conduction in the wall as can be seen in Figure 2. In a steady state situation the temperature gradient inside the wall is linear. In that case the one dimensional Fourier's law (2) can be expressed as

$$\Phi''_{\text{wall}} = -k_{\text{wall}} \frac{\Delta T_{\text{wall}}}{s_{\text{wall}}}, \tag{4}$$

where ΔT_{wall} is the temperature difference in the wall and s_{wall} is the thickness of the wall.

If convection is included, it will make the situation a little bit more complicated. The fluid is receiving or releasing heat depending on the side of the wall. When the fluid is flowing along the wall, the temperature of the fluid is changing as well as the surface temperature of the wall in different places of the surface. Next, heat transfer through a wall in one point of the intersection of the wall will be studied. If we combine convection and conduction at one point on the wall, we will obtain the following equation for heat flux

$$\Phi'' = U(T_{\text{h}_\infty} - T_{\text{c}_\infty}) = U\Delta T_{\infty}, \tag{5}$$

where

U	is the overall heat transfer coefficient	[W/m^{2}K],

T_{h_∞}	is the temperature of hot flow in the mixed layer	[°C],
T_{c_∞}	is the temperature of cold flow in the mixed layer	[°C],
ΔT_∞	is the temperature difference between the hot and the cold mixed layers	[°C].

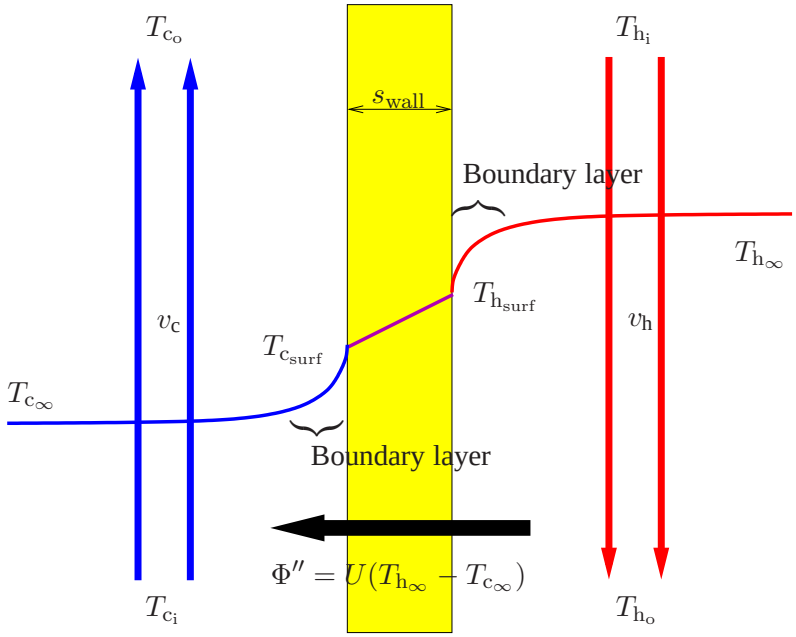

Figure 2: Transfer of heat through the wall

The overall heat transfer coefficient combines conduction and convection resistances between fluids in the following way

$$\frac{1}{U} = \frac{1}{\alpha_{\mathrm{h}}} + \frac{s_{\mathrm{wall}}}{k_{\mathrm{wall}}} + \frac{1}{\alpha_{\mathrm{c}}}, \tag{6}$$

where α_{h} is the convective heat transfer coefficient on the hot side and α_{c} is the convective heat transfer coefficient on the cold side [2, pp. 80-85]. The wall has a minor effect on the overall heat transfer coefficient and thus the central term on the right hand side of the equation can be neglected.

The convective heat transfer coefficient α for fluid can be solved from the definition of the Nusselt number

$$\mathrm{Nu} = \frac{\alpha d_{\mathrm{hydr}}}{k}, \tag{7}$$

where

Nu	is the Nusselt number	[-],
d_{hydr}	is the case specific hydraulic diameter	[m],
k	is the thermal conductivity of the fluid	[W/mK].

Nusselt number describes thermal gradient in a boundary layer. There are several empirical correlations for Nusselt number in literature. We use the Dittus–Boelter correlation here for turbulent flow in circular tubes [2, p. 496]. The equation for this situation is

$$\mathrm{Nu} = C\mathrm{Re}^m\mathrm{Pr}^n, \tag{8}$$

where

C, m and n	are the experimental constants for the Nusselt number	[-],
Re	is the Reynold's number	[-],
Pr	is the Prandlt number	[-].

Reynold's number is a measure of turbulence in the flow. Its definition is

$$\mathrm{Re} = \frac{v\rho d_{\mathrm{hydr}}}{\mu}, \tag{9}$$

where

v	is the velocity of the fluid	[m/s]
ρ	is the density of the fluid	[kg/m^3],
μ	is the dynamic viscosity of the the fluid	[Ns/m^2].

Prandtl number describes dimensionless viscosity of the fluid. Its definition is

$$\mathrm{Pr} = \frac{c_p\mu}{k}, \tag{10}$$

where c_p is the specific heat capacity of the fluid.

2.3 Model of the heat exchanger without phase change

A heat exchanger can be constructed of tubes or plates. We derive the model for a cross-flow plate heat exchanger.

The heat flux can be written as

$$\Phi'' = \frac{\Phi}{A}, \tag{11}$$

where Φ is the heat rate and A is the heat surface area.

The heat rate is obtained by integrating equation (5) with respect to the surface area

$$\Phi = \int_A \mathrm{d}\Phi = \int_A U \Delta T_\infty \mathrm{d}A\,. \tag{12}$$

We obtain

$$\Phi = UA\Delta T_{\mathrm{lm}}, \tag{13}$$

where ΔT_{lm} is the logarithmic mean temperature difference between the hot and the cold side. For the counterflow heat exchanger we get

$$\Delta T_{\mathrm{lm}} = \frac{\Delta T_2 - \Delta T_1}{\ln \frac{\Delta T_2}{\Delta T_1}} = \frac{(T_{\mathrm{h_o}} - T_{\mathrm{c_i}}) - (T_{\mathrm{h_i}} - T_{\mathrm{c_o}})}{\ln \frac{(T_{\mathrm{h_o}} - T_{\mathrm{c_i}})}{(T_{\mathrm{h_i}} - T_{\mathrm{c_o}})}}, \tag{14}$$

where

$T_{\mathrm{h_i}}$	is the temperature of hot inlet flow	[°C],
$T_{\mathrm{c_i}}$	is the temperature of cold inlet flow	[°C],
$T_{\mathrm{h_o}}$	is the temperature of hot outlet flow	[°C],
$T_{\mathrm{c_o}}$	is the temperature of cold outlet flow	[°C].

Logarithmic mean temperature difference combines local temperature differences in different places over the heat exchanger. Derivation of logarithmic mean temperature difference is given in [2, pp. 646-649].

For a cross-flow heat exchanger the heat rate is written as

$$\Phi = FUA\Delta T_{\mathrm{lm}}. \tag{15}$$

Here F is the *correction factor* which corrects ΔT_{lm} for the cross-flow heat exchanger.

The formula for the factor is

$$F = \begin{cases} (1+0.9\xi^2)^{-0.15} & \xi \leq 2 \\ \dfrac{\sqrt{\pi\xi}}{\xi - 0.0625} - \dfrac{1}{\xi} & \xi > 2 \end{cases}, \tag{16}$$

where ξ is the auxiliary variable in the calculation of F, see [4, Ca 7].

For a one pass heat exchanger the variable ξ can be calculated by the equation

$$\xi = Z_{\mathrm{h}} \left(0.6\sqrt{R_{\mathrm{h}}} + \frac{0.8R_{\mathrm{h}}}{1+R_{\mathrm{h}}} \right), \tag{17}$$

where Z_{h} is the number of transfer units and R_{h} is the heat capacity flow ratio.

When combining heat exchanger units for multi-pass mixed cold flow and unmixed hot flow the expression for ξ becomes

$$\tilde{\xi} = \sqrt{R_{\mathrm{h}}} \frac{Z_{\mathrm{h}}}{n_{\mathrm{pass}}}, \tag{18}$$

where $\tilde{\xi}$ is the auxiliary variable in the calculation of $F_{\mathrm{n_{pass}}}$ in one pass and n_{pass} is the number of passes in combined heat exchanger unit [4, Ca 9].

In a multipass case, the correction factor is calculated by formula

$$F_{\mathrm{n_{pass}}} = \frac{1}{n_{\mathrm{pass}}} F_1 + \frac{n_{\mathrm{pass}} - 1}{n_{\mathrm{pass}}} F_\infty \tag{19}$$

using the variable $\tilde{\xi}$ in equation (16) instead of the variable ξ for the factor F_1. The factor F_∞ is calculated as

$$F_\infty = (1 + 0.63\tilde{\xi}^2)^{-0.24}. \tag{20}$$

Equation (18) was used instead of equation (17) also for one pass heat exchanger because the results did not differ a lot. Actually in this thesis only one pass heat exchangers were used.

The number of transfer units or dimensionless conductance is denoted by the equation

$$Z_{\mathrm{h}} = \frac{UA}{q_{m_{\mathrm{h}}} c_{p_{\mathrm{h}}}}, \tag{21}$$

where $q_{m_{\mathrm{h}}}$ is the mass flow of the hot fluid and $c_{p_{\mathrm{h}}}$ is the specific heat capacity of the hot inlet flow. Heat capacity flow ratio is denoted by the equation

$$R_{\mathrm{h}} = \frac{q_{m_{\mathrm{h}}} c_{p_{\mathrm{h}}}}{q_{m_{\mathrm{c}}} c_{p_{\mathrm{c}}}}, \tag{22}$$

where $q_{m_{\mathrm{c}}}$ is the mass flow of the cold fluid and $c_{p_{\mathrm{c}}}$ is the specific heat capacity of the cold inlet flow.

The overall heat transfer coefficient U also varies along the heat exchanger with the change of temperature due to changing values of material properties as will be explained later in Section 3.2.3. Therefore it is important to use the global correlation in equation (8) instead of a local one.

In equation (15) there are three unknowns: the heat rate Φ, the outlet temperature $T_{\mathrm{h_o}}$ on the hot side and the outlet temperature $T_{\mathrm{c_o}}$ on the cold side. To solve the unknowns the heat exchanger has to be studied along the flows of the fluids on both sides. Here we need the law of energy conservation. When cold air passes through the heat exchanger it is warmed up. It receives all the energy which is passed through the wall from the hot side, because we assume that the unit is perfectly insulated and in a steady state situation the wall cannot reserve any energy. The amount of energy received by the fluid is proportional to the temperature difference between the outlet and the inlet. In general the amount of energy needed to heat any material is

$$Q = mc_p \Delta T, \tag{23}$$

where

Q	is the energy	[J],
m	is the mass	[kg],
ΔT	is the temperature difference	[°C].

The heating power is obtained by dividing equation (23) with unit time Δt. Thus the heat

rate on the cold side is denoted by the equation

$$\Phi = q_{m_\mathrm{c}} c_{p_\mathrm{c}} (T_{\mathrm{c_o}} - T_{\mathrm{c_i}}). \tag{24}$$

In the same way, a hot fluid is loosing heat energy with the same power as a cold fluid is receiving that. So the equation for heat rate on the hot side is

$$\Phi = q_{m_\mathrm{h}} c_{p_\mathrm{h}} (T_{\mathrm{h_i}} - T_{\mathrm{h_o}}). \tag{25}$$

By combining equations (24), (25) and (15) we will obtain the following model for the cross-flow heat exchanger:

$$\begin{cases} \Phi &= q_{m_\mathrm{h}} c_{p_\mathrm{h}} (T_{\mathrm{h_i}} - T_{\mathrm{h_o}}), \\ \Phi &= q_{m_\mathrm{c}} c_{p_\mathrm{c}} (T_{\mathrm{c_o}} - T_{\mathrm{c_i}}), \\ \Phi &= FUA\Delta T_{\mathrm{lm}}. \end{cases} \tag{26}$$

For a given heat exchanger, the independent known variables are $T_{\mathrm{h_i}}$ and $T_{\mathrm{c_i}}$. The outlet temperatures $T_{\mathrm{h_o}}$ and $T_{\mathrm{c_o}}$ are the state variables to be computed by solving the system in equation (26). Note that (26) forms a nonlinear pair of equations. It has to be solved numerically.

The *mechanical dimensioning problem* is an optimisation problem where we try to minimise area A and maximise heat rate Φ, while keeping the outlet temperatures inside the required boundary conditions. Regardless of whether we are dealing with a mechanical dimensioning problem or an existing heat exchanger, Φ is always the most interesting variable from the practical point of view.

2.4 Model of the condensing surface heat exchanger

The heat of vaporisation and thus the energy released in the condensation of water vapour is much more than energy released from water vapour alone in the typical temperature change for heat exchangers. The amount of the energy released in the condensation can

exceed the amount of the energy received in the temperature change of moist air. If there occurs a phase change in the heat exchanger, the results of the model without phase change are no more valid. Condensation starts when the surface temperature T_{surf} drops below the dew point T_{dew}. As far as this does not happen it is safe to use the model without phase change.[1]

The condensing surface model is more demanding than the model without phase change because the mass transfer of the condensate has to be taken into account in addition to heat transfer. For a condensing case a model derived by Soininen [5] will be used. It is based on the mechanical dimensioning problem, where the area A is not known because the heat exchanger does not yet exist. His model solves the area, which is needed to heat the cold fluid to the desired temperature, when the incoming temperatures are known. The incoming temperatures $T_{\mathrm{h_i}}$ and $T_{\mathrm{c_i}}$ and the outgoing cold temperature $T_{\mathrm{c_o}}$ are given while area A and hot outgoing temperature $T_{\mathrm{c_o}}$ are unknowns. The model is consisting of a group of differential equations. The model and the main idea to implement that as a computer program will be described here. For more details see [5].

Figure 3 illustrates the heat and the mass balances of an element $\mathrm{d}A$ on the condensing surface of the heat exchanger. Hot air and condensate are flowing downwards on the right hand side of the surface and cold fluid upwards on the left side of the surface. Dashed line in the condensate separates new condensate formed in the studied area element and old condensate flowing downwards.

Similarly as in equation (6), the overall heat transfers coefficient can be defined as

$$\frac{1}{\alpha_{\mathrm{k}}} = +\frac{1}{\alpha_{\mathrm{c}}} + \frac{s_{\mathrm{wall}}}{k_{\mathrm{wall}}} + \frac{1}{\alpha_{\mathrm{w}}}, \tag{27}$$

where α_{k} is the overall heat transfers coefficient from the condensate to the cold flow and α_{w} is the convective heat transfer coefficient of the condensate (water). The wall and condensate has a minor effect on the overall heat transfer coefficient and can be neglected, thus $\alpha_{\mathrm{k}} \approx \alpha_{\mathrm{c}}$.

[1] In a cross-flow heat exchanger there is always a temperature profile in the outlets as can be seen in Figure 6 for reasons described in page 27. Because the solution of the model without phase change is mean temperature of the outlet, there has to be some safety marginals for surface temperature not to drop below dew point.

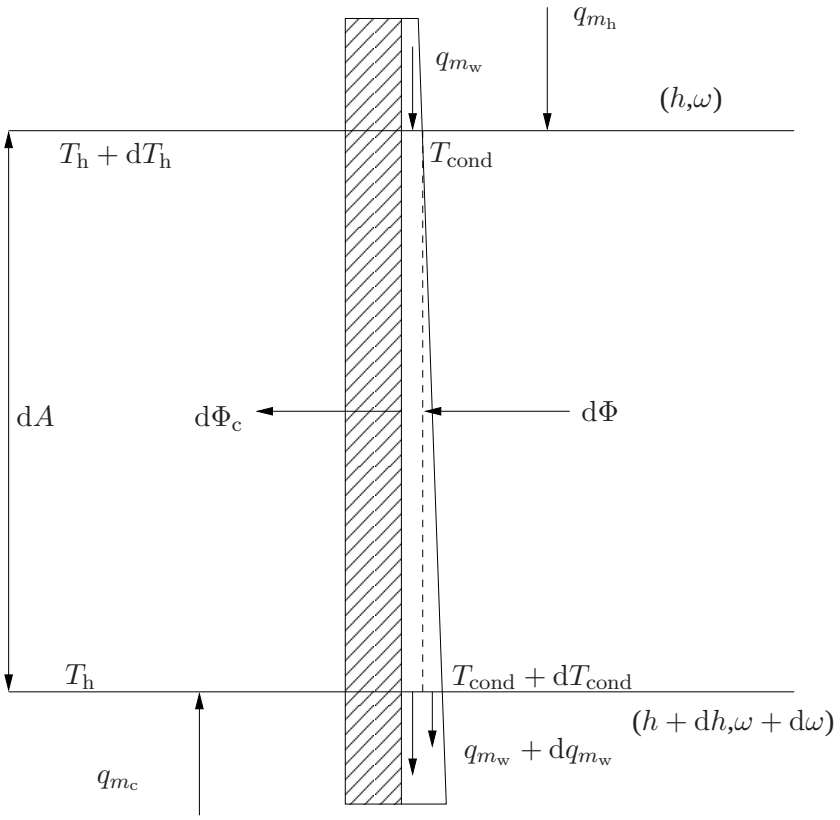

Figure 3: An illustration of the heat and mass balance on the condensing surface. New condensate $\mathrm{d}q_{m_\mathrm{w}}$ is formed on the surface element $\mathrm{d}A$ on the right hand side of dashed line in condensate. Arrows indicate the direction of the flow.

Let us examine the the volume element on the right hand side of the dashed line in the condensate in Figure 3. The heat balance for the volume element can be written by

$$\mathrm{d}\Phi + q_{m_\mathrm{h}}\mathrm{d}h + c_{p_\mathrm{w}}T_\mathrm{cond}\mathrm{d}q_{m_\mathrm{w}} = 0, \tag{28}$$

where

q_{m_h}	is the mass flow of the hot air	[kg/s],
h	is the specific enthalpy of the moist air	[J/kg],
c_{p_w}	is the specific heat capacity of the condensate (water)	[J/kgK],
T_cond	is the temperature of the condensated water	[°C],
q_{m_w}	is the mass flow of the condensate (water)	[kg/s].

The mass balance for the volume element can be written by

$$\mathrm{d}q_{m_\mathrm{w}} + q_{m_\mathrm{h}}\mathrm{d}\omega = 0, \tag{29}$$

where ω is the moisture content of the air.

The differential for the enthalpy of the moist air in the volume element is given by

$$\mathrm{d}h = (c_{p_{\mathrm{da}}} + \omega c_{p_{\mathrm{wv}}})\mathrm{d}T_{\mathrm{h}} + (r_0 + c_{p_{\mathrm{wv}}} T_{\mathrm{h}})\mathrm{d}\omega, \tag{30}$$

where

$c_{p_{\mathrm{da}}}$	is the specific heat capacity of dry air	[J/kgK],
$c_{p_{\mathrm{wv}}}$	is the specific heat capacity of water vapour	[J/kgK],
T_{h}	is the temperature of the moist air in the hot side	[°C],
r_0	is the heat of vaporisation at 0 °C	[2501 J/kg].

Substituting equation (29) and equation (30) in equation (28) yields

$$\mathrm{d}\Phi = -q_{m_{\mathrm{h}}}(c_{p_{\mathrm{da}}} + \omega c_{p_{\mathrm{wv}}})\mathrm{d}T_{\mathrm{h}} + (r_0 + c_{p_{\mathrm{wv}}} T_{\mathrm{h}} - c_{p_{\mathrm{w}}} T_{\mathrm{cond}})\mathrm{d}q_{m_{\mathrm{w}}}. \tag{31}$$

The first term on the right hand side of equation (31) is given by

$$-q_{m_{\mathrm{h}}}(c_{p_{\mathrm{da}}} + \omega c_{p_{\mathrm{wv}}})\mathrm{d}T_{\mathrm{h}} = \alpha_{\mathrm{cond}}(T_{\mathrm{h}} - T_{\mathrm{cond}})\mathrm{d}A, \tag{32}$$

where α_{cond} is the convective heat transfer coefficient during a simultaneous mass transfer.

The differential for the mass flow of the condensate is obtained by

$$\mathrm{d}q_{m_{\mathrm{w}}} = \frac{\alpha_{\mathrm{cond}}}{c_{p_{\mathrm{da}}} + \omega_{\mathrm{cond}} c_{p_{\mathrm{wv}}}}(\omega - \omega_{\mathrm{cond}})\mathrm{d}A, \tag{33}$$

where ω_{cond} is the moisture content of saturated air. When substituting equation (33) in equation (31) we obtain

$$\begin{aligned} \mathrm{d}\Phi &= \frac{\alpha_{\mathrm{cond}}}{c_{p_{\mathrm{da}}} + \omega_{\mathrm{cond}} c_{p_{\mathrm{wv}}}}[(c_{p_{\mathrm{da}}} + \omega_{\mathrm{cond}} c_{p_{\mathrm{wv}}})(T_{\mathrm{h}} - T_{\mathrm{cond}}) \\ &\quad + (r_0 + c_{p_{\mathrm{wv}}} T_{\mathrm{h}} - c_{p_{\mathrm{w}}} T_{\mathrm{cond}})(\omega - \omega_{\mathrm{cond}})]\mathrm{d}A \\ &= \alpha_{\mathrm{cond}} \left[\frac{h - h_{\mathrm{cond}}}{c_{p_{\mathrm{da}}} + \omega_{\mathrm{cond}} c_{p_{\mathrm{wv}}}} - \frac{\omega - \omega_{\mathrm{cond}}}{c_{p_{\mathrm{da}}} + \omega_{\mathrm{cond}} c_{p_{\mathrm{wv}}}} c_{p_{\mathrm{w}}} T_{\mathrm{h}}\right] \mathrm{d}A \end{aligned} . \tag{34}$$

where h_{cond} is the specific enthalpy of the condensate.

Equation for the Θ-function is

$$\Theta = \Theta_h - \Theta_\omega, \tag{35}$$

where Θ_h is the Θ-function of enthalpy and Θ_ω is the Θ-function of moisture content. The equation for the Θ_h-function is given as

$$\Theta_h = \frac{h - h_{\mathrm{cond}}}{c_{p_{\mathrm{da}}} + \omega_{\mathrm{cond}} c_{p_{\mathrm{wv}}}} \tag{36}$$

and for the Θ_ω-function reads as

$$\Theta_\omega = \frac{\omega - \omega_{\mathrm{cond}}}{c_{p_{\mathrm{da}}} + \omega_{\mathrm{cond}} c_{p_{\mathrm{wv}}}} c_{p_{\mathrm{w}}} T_{\mathrm{cond}}. \tag{37}$$

Substituting equations (36) and (37) in equation (34) yields

$$\mathrm{d}\Phi = \alpha_{\mathrm{cond}}(\Theta_h - \Theta_\omega)\mathrm{d}A = \alpha_{\mathrm{cond}}\Theta \mathrm{d}A. \tag{38}$$

Equations (33) and (38) holds true under the assumption

$$\frac{\mathrm{d}h}{\mathrm{d}\omega} = \frac{h - h_{\mathrm{cond}}}{\omega - \omega_{\mathrm{cond}}}. \tag{39}$$

For the the volume element between the heat surface and the dashed line in the condensate in Figure 3 the heat balance is

$$\mathrm{d}\Phi_{\mathrm{c}} = \mathrm{d}\Phi - q_{m_{\mathrm{w}}} c_{p_{\mathrm{w}}} \mathrm{d}T_{\mathrm{cond}}, \tag{40}$$

where Φ_{c} is the heat rate on the cold side.

Finally we examine the volume element on the supply side of the heat exchanger. As in equation (24) for the model without phase change the heat balance for condensing surface model in the volume element is

$$\mathrm{d}\Phi_{\mathrm{c}} = q_{m_{\mathrm{c}}} c_{p_{\mathrm{c}}} \mathrm{d}T_{\mathrm{c}}, \tag{41}$$

where T_c is the temperature of the fluid in the cold side. As in equation (13) for the heat exchanger model without phase change the heat balance for condensing surface model in the volume element is

$$\mathrm{d}\Phi_\mathrm{c} = \alpha_\mathrm{k}(T_\mathrm{cond} - T_\mathrm{c})\mathrm{d}A. \tag{42}$$

To be able to solve the temperature of the condensate T_cond we combine equations from equation (38) to equation (42). If we then divide the result with $\alpha_\mathrm{cond}\mathrm{d}A$ we will obtain

$$\frac{\alpha_\mathrm{k}}{\alpha_\mathrm{cond}}(T_\mathrm{cond} - T_\mathrm{c}) = \Theta - \frac{q_{m_\mathrm{w}} c_{p_\mathrm{w}}}{\alpha_\mathrm{cond}} \frac{\mathrm{d}T_\mathrm{cond}}{\mathrm{d}A}. \tag{43}$$

The last term of equation (43) is usually of minor magnitude and thus often the last term can be neglected [5, p. 878]. Doing so we end up shorter equation:

$$\frac{\alpha_\mathrm{k}}{\alpha_\mathrm{cond}}(T_\mathrm{cond} - T_\mathrm{c}) = \Theta. \tag{44}$$

According to Soininen, there is more than one way of creating a computer program for analysing the process and the area of the heating surface [5, p. 879]. The one used here is the same as in his article. Soininen discretised the differential equations described above and formed a group of difference equations.

We examine a countercurrent heat exchanger, where hot air is flowing downwards and cold fluid upwards. The heat exchanger is divided into N cells according to Figure 4. There is no phase change on the cold side, thus the heat rate on the cold side Φ_c can be calculated as in (24). The discretisation is designed so that the areas of the cells are varying but the heat rates $\Delta\Phi_\mathrm{c}$ through the cells are equal among all cells and thus also the temperature difference ΔT_c of a cell on the cold side can be calculated. Indices a and b are for boundaries of the cell according to the flow direction of the hot side as in Figure 4.

The computation starts from the uppermost cell. For the cold side all incoming and outgoing flow values are known in every cell. For the uppermost cell that is also true for the hot incoming air but not for the outgoing air. The edge a of the uppermost cell is set to point where the condensation starts. There is no condensate coming in before that. There can be dry, noncondensing surface before the condensation starts but it can be solved using the model without phase change. The temperature of the condensate T_cond at the point where the condensation starts can be solved from equation (44).

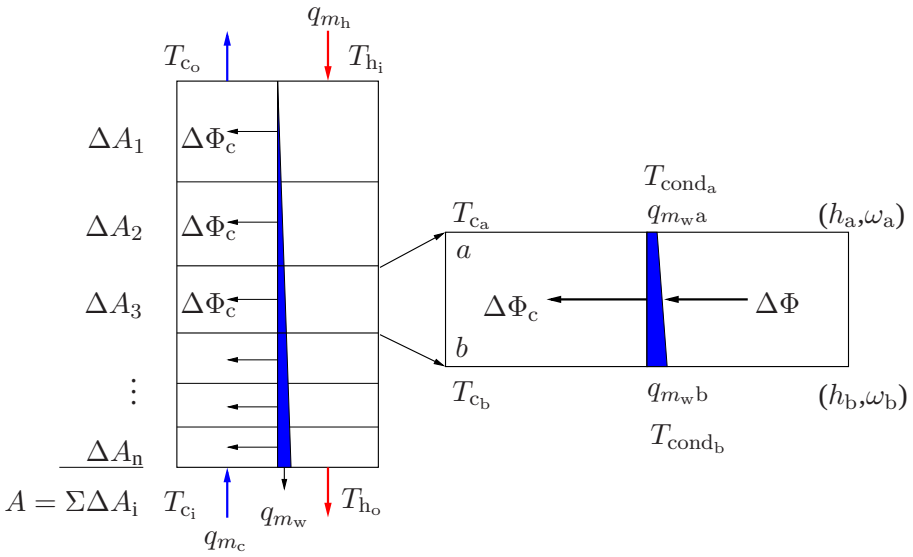

Figure 4: An illustration of the condensing surface model. Arrows indicate the direction of the flow. Red arrow is hot air and blue arrow is cold air. Blue wedge is condensed water.

As stated in [5, p. 881], when for a certain section, the values of h_a, ω_a, $q_{m_\mathrm{w}\mathrm{a}}$, $T_{\mathrm{cond_a}}$ and $T_{\mathrm{c_a}}$at the boundary a are known, the five unknown quantities $\Delta\Phi$, ΔA, ΔT_cond, Δh and $\Delta\omega$ (see Figure 4) can be solved from a group of the five equations:

$$\begin{cases} \Delta\Phi = q_{m_\mathrm{h}}\left(\Delta h - c_{p_\mathrm{w}}(T_{\mathrm{cond_a}} - \Delta T_\mathrm{cond})\Delta\omega\right), \\ \Delta\Phi = \alpha_\mathrm{cond}\bar{\Theta}\Delta A, \\ \Delta\Phi_\mathrm{c} = \Delta\Phi + q_{m_\mathrm{w}\mathrm{a}}c_{p_\mathrm{w}}\Delta T_\mathrm{cond} = q_{m_\mathrm{c}}c_{p_\mathrm{c}}\Delta T_\mathrm{c}, \\ \Delta\Phi_\mathrm{c} = \alpha_\mathrm{k}(T_{\mathrm{cond_a}} - \Delta T_\mathrm{cond}/2 - T_{\mathrm{c_i}} + \Delta T_\mathrm{c}/2)\Delta A, \\ \Delta q_{m_\mathrm{w}} = q_{m_\mathrm{h}}\Delta\omega = \dfrac{\alpha_\mathrm{cond}}{2}\left(\dfrac{\omega_\mathrm{a} - \omega_{\mathrm{cond_a}}}{c_{p_\mathrm{da}} + \omega_{\mathrm{cond_a}}c_{p_\mathrm{wv}}} + \dfrac{\omega_\mathrm{a} - \Delta\omega - \omega_{\mathrm{cond_b}}}{c_{p_\mathrm{da}} + \omega_{\mathrm{cond_b}}c_{p_\mathrm{wv}}}\right)\Delta A, \end{cases} \tag{45}$$

where $\bar{\Theta}$ is the mean value of the Θ-function at cell boundaries a and b.

Soininen did not reduce the difference equation group. However, as in the heat exchanger model (26) without phase change the system can be reduced further. So we arrive at a system of three equations, from which the three unknowns can be solved.

The outgoing values for the cell can be approximated by solving the system (45) and adding the results to inlet values for the cell. Once the outgoing values are calculated the incoming values for the next cell are got by substituting the outgoing values for the incoming ones. Then the process is repeated for every cell. At the end the value for the heat exchanger area can be calculated as a sum of the areas of the cells.

If the cold fluid is heated above the dew point of the hot air so that the surface temperature is above the dew point, the upper part of the heat exchanger will be noncondensing. The dry area can be solved by equation (13) so that Φ is the heat rate through the dry part. That can be solved by

$$\Phi_{\mathrm{dry}} = \frac{\alpha_{\mathrm{cond}} T_{\mathrm{h_i}} + \alpha_{\mathrm{k}} T_{\mathrm{c_o}} - (\alpha_{\mathrm{cond}} + \alpha_{\mathrm{k}}) T_{\mathrm{dew}}}{\frac{\alpha_{\mathrm{cond}}}{q_{m_{\mathrm{h}}} c_{p_{\mathrm{ma}}}} + \frac{\alpha_{\mathrm{k}}}{q_{m_{\mathrm{c}}} c_{p_{\mathrm{c}}}}}, \tag{46}$$

where

Φ_{dry}	is the heat rate of the dry part	[W],
T_{dew}	is the dew point of the moist air	[°C],
$c_{p_{\mathrm{ma}}}$	is the specific heat capacity of moist air	[J/kgK].

The dew point temperature can be calculated by

$$p_{\mathrm{wv}} = \omega \frac{p_{\mathrm{s}}}{\omega + 0.62197} \tag{47}$$

and

$$T_{\mathrm{dew}} = 99.64 + 329.64 \frac{\ln(p_{\mathrm{wv}})}{11.78 + \ln(p_{\mathrm{wv}})}, \tag{48}$$

where p_{wv} is the water vapour pressure and p_{s} is the static pressure.

To summarise, the condensing case leads to a system where a nonlinear system of equations for three unknowns has to be solved at each discretisation step. The effect of the number of discretisation steps to the accuracy of the result will be studied in Section 7.3. This mechanical dimensioning problem where the area is unknown can be changed to the problem of existing heat exchanger and known area. That is done by solving the condensing surface model again and again and varying the cold outlet fluid temperature until the calculated area of the solution reaches the desired area. In the problem of existing heat exchanger three unknown state variables are $T_{\mathrm{h_o}}$, $T_{\mathrm{c_o}}$ and ω_{h}. The last of those is not usually measured directly, but calculated with the wet bulk temperature as described later in Section 3.2.2.

3 Model variables

Most of the variables in equation (26) are calculated by measured variables, which will be discussed in Section 3.1. Model variables calculated with directly measured variables will be discussed in Section 3.2. Only the temperatures in equation (26) are measured directly. They can be given either in Kelvins or in Celsius degrees because we are dealing with temperature differences. In Appendix 1 the formulas for material properties will be given either in Kelvins or Celsius degrees depending on the equation. Later the temperature will always be given in Celsius degrees if not mentioned otherwise.

3.1 Measured variables

In this section we will discuss the measured or observed variables when the fluid is air. Then the measured variables are the dry bulb temperature T_{dry}, the wet bulb temperature T_{wet}, atmospheric pressure p_{atm}, dynamic pressure p_{d} of the flow and the pressure difference Δp between the inside and the outside of the ventilation duct. All measurements are done on both sides of the heat exchanger, on the cold and on the hot side. The atmospheric pressure simply is assumed to be the same everywhere. A typical example of the measurements in the moist air cross-flow heat exchanger is given in Figure 5.

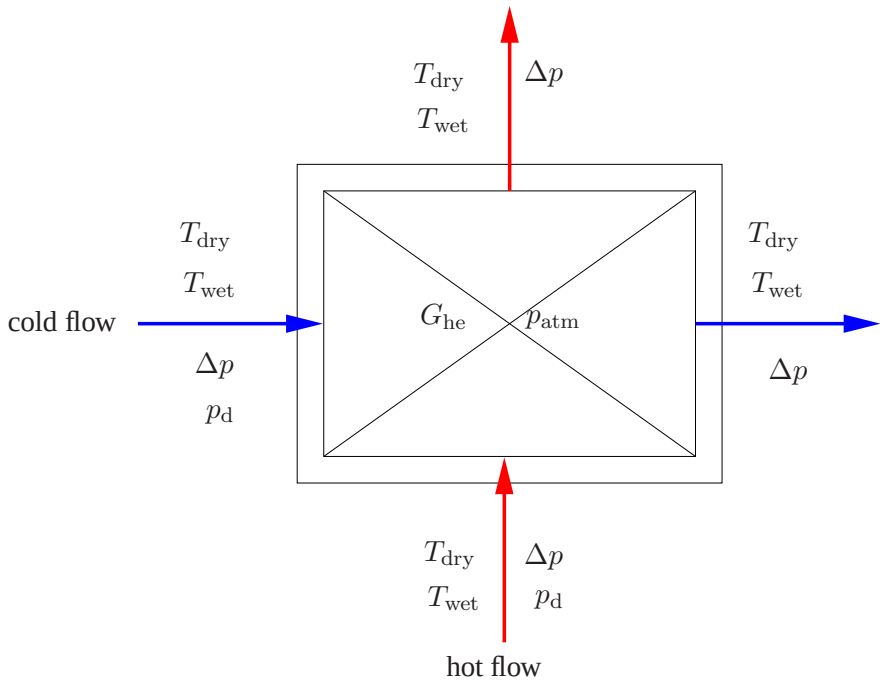

Figure 5: Measurements in moist air cross-flow heat exchanger.

The area and the other geometry information of the heat exchanger is received from the manufacturer. The area of the ventilation duct, which is used in the calculation of mass flow, is measured and rounded to the nearest manufactured standard value or reasonable value.

Sometimes the pressure difference between the inside and the outside of the ventilation duct can be called the static pressure. Here the static pressure is denoted by p_{s} and it is the sum of the atmospheric pressure and the pressure difference between the inside and the outside of the duct, $p_{\mathrm{s}} = \Delta p + p_{\mathrm{atm}}$. It is equal to the pressure inside the ventilation duct. The usage of the word total pressure instead of static pressure is avoided because it can be confused with the total pressure in Bernoulli equation, $p_{\mathrm{tot}} = p_{\mathrm{s}} + p_{\mathrm{d}}$.

The model variables are divided into calculated and measured variables because later in Section 6.4 also the error variance of the independent control variables will be considered. There the error will be added to the originally measured variables. Assumptions about error levels are based on the measurement accuracy. That will be studied next more carefully.

3.1.1 Measuring and measurement inaccuracy

There are several sources of errors in the measuring process. On site measurement error is larger than the error in laboratory conditions. Manufacturers give information about the error of a measuring instrument in laboratory conditions. The form of informing the measurement error has not been standardised in any way. Usually the result of laboratory measurement is compared to a result, which has been measured with a more accurate instrument. The measuring instrument will be accepted if the result is within error limits. Such a procedure implies univariate measurement error [6]. However, all measurement errors in thesis are considered as Gaussian and homoscedastic even thought in practice they are mostly heteroscedastic.

All measurements are done on both the cold and the hot side of the heat exchanger. The measurements can be done either before the inlet or after the outlet or both. The measurements are usually not made on-line and in practice measuring one unit takes approximately half an hour. All measurements are done on one side of the unit at a time. It is possible that circumstances vary a bit between the measurements, which is one possible source of error. Lot of measuring information and the error approximations in the next pages are based on [7].

Dry bulb temperatures are measured at only one point on each four sides of the heat exchanger (hot and cold, inlet and outlet). The temperature measurements are done by PT100-sensors, which are based on the fact that electric resistance is a function of temperature. The accuracy of thermometers is usually near 0.1°C at 0°C and the error is heteroscedastic — increasing with temperature. The standard deviation (std) of the strict error in the thermometer alone is assumed to be $\sigma = 0.025$°C.

The temperatures are measured at one depth inside the ventilation duct from one hole, which is in the middle of the wall of a square ventilation duct. In the outlet, after the heat exchanger, the fluid has a temperature profile that can be seen in Figure 6. The temperature profile is formed because on one side of the heat exchanger hot air is facing the coldest possible air all the time. On the other side the cold air is heated before it reaches hot air. In one paper mill, for example, some temperatures in the outlet profiles were measured. The measured values for one heat exchanger outlet profile were 46.8°C, 48.4°C and 52.3°C. The internal temperature difference of the temperature profile in one outlet was approximately 4°C. The temperature values in equation (26) are mean values.

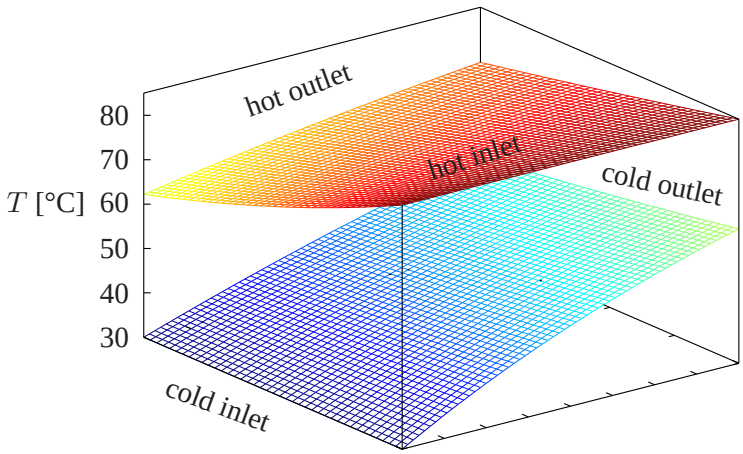

Figure 6: Temperature profiles inside the cross-flow heat exchanger. The upper surface is the hot side and the lower surface is the cold side.

The sensors are short and do not reach the centre of the duct. They can point in different directions if the measurement is repeated and thus they will measure a different point of the temperature profile. Temperature profile can change depending on the flow conditions. Especially, in the outlets this can be one main source of error in addition to instrument error. It takes some time for the sensor to reach the temperature of the fluid as can be seen in the solid lines of Figure 7. If the reading is read too soon, it will cause a systematic error. If the measuring was repeated, there would be some extra random error, too. That

would be caused in addition to normal random error because it would be impossible to read the reading exactly at the same time as previously. So the real measurement error will be much larger than the error caused by the thermometer alone. For the error in dry bulb temperatures $\sigma = 0.25$°C has been used as a standard deviation.

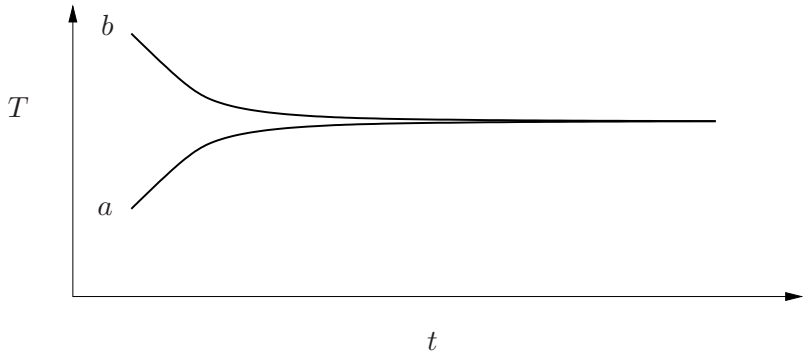

Figure 7: Readings from the sensors during the dry bulb temperature measurements. Label a points to case where the sensor is colder than the target of the measurement in the beginning of the measurement process. Label b points to case where the sensor is warmer than the target of the measurement in the beginning of the measurement process. The correct dry bulb temperature is measured in the area where the readings are stabilised.

Wet bulb temperature is measured at the same time as dry bulb temperature with a similar sensor. In the wet bulb temperature measurement the sensor is covered with a cloth rinsed in clean water. When water starts to evaporate from the cloth, it cools down the sensor compared to the sensor which is measuring the dry bulb temperature. The drier the air is, the larger is the difference between the dry and the wet bulb temperatures. When the cloth becomes dry enough, the sensor which is measuring the wet bulb temperature starts to warm up until it reaches the temperature of the dry sensor.

If the wet cloth is colder than the wet bulb temperature, the temperature of the sensor measuring the wet bulb temperature will increase until it reaches the dry bulb temperature. One tries to read the wet bulb temperature at the moment when the temperature is stable. That can be seen as a flat part in Figure 8. If the air is very dry and hot and the velocity of the flow is high, the reading can be very difficult, because flat part is very short. If the wet cloth is warmer than the wet bulb temperature, first the sensor starts to cool down and then to warm up. One tries to read the temperature in the inflection point. Measurement error is larger in the first case and it is larger than the measurement error of the dry bulb temperature in all cases. The error in measuring the wet bulb temperature is the function of the flow rate and the humidity. Standard deviation $\sigma = 0.5$°C is used here as a value for the error in the wet bulb temperatures.

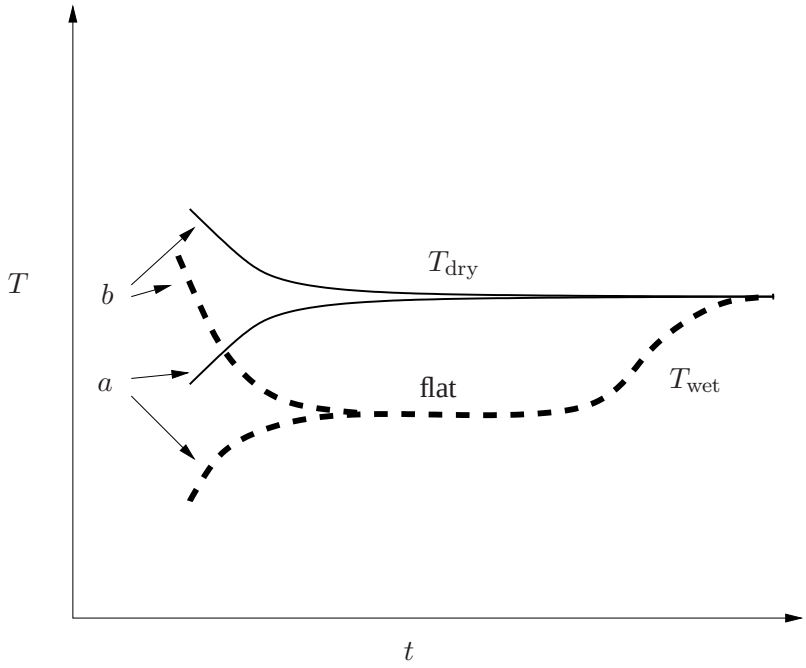

Figure 8: Readings from the sensors during the dry and wet bulb temperature measurements. The solid line represents the dry bulb temperature and the dashed line represents the wet bulb temperature. Label a points to cases where the sensor is colder than the target of the measurement in the beginning of the measurement process. Label b points to cases where the sensor is warmer than the target of the measurement in the beginning of the measurement process. The correct wet bulb temperature is measured in the flat area of the figure.

The same pressure gauge is used to measure both the dynamic pressure and the pressure difference between the inside and the outside of the ventilation duct. The values for the pressure difference and the dynamic pressure are usually some hundreds of Pascals or less. The pressure difference is measured from one point in every side of the heat exchanger. For example, the Macnehelic gauge of Dwyer Instruments has an error below $\pm 2\%$ of the full scale. Standard deviation $\sigma = 1$ Pascals is used here as a value for the error in the pressure difference.

The dynamic pressure is measured through a Pitot static-tube. That is put through the wall of the ventilation duct so that the tip of the tube is pointing towards the incoming fluid flow. The dynamic pressure is the pressure difference between the pressure caused by the flow of fluid in the tip of the Pitot tube and the pressure inside the duct in a calm, sheltered place. Unlike other measurements dynamic pressure is measured at several points of the cross section of the ventilation duct, so that the measurement points form a grid [8]. The dynamic pressure is usually measured at the inlets only.In practice the error of the dynamic pressure should always exceed the error of the pressure difference between the

inside and the outside of the duct if they are measured with the same pressure gauge. In the same way, the error of wet bulb temperature is always larger than the error of the dry bulb temperature. Standard deviation $\sigma = 2.5$ Pascals is used here as a value for the error in the dynamic pressure.

The atmospheric pressure measurements are usually got from the nearest weather station or airport. One has to make an altitude correction, because the atmospheric pressures are announced in the sea level. The error of the barometer is less than 50 Pascals. However, the normal atmospheric pressure, 101325 Pascals, is often assumed without making any measurements. In that case the error in the atmospheric pressure can exceed 1000 Pascals depending on the weather. In Nauvo, Finland, for example, the atmospheric pressure was measured twice an hour for a year and the standard deviation was over 1000 Pascals [9]. Standard deviation $\sigma = 1000$ Pascals is used here as a value for the error in the atmospheric pressure measurements. In Table 2 there are collected all measurement errors used in thesis.

Table 2: Standard deviations σ of the measurement errors used in the thesis.

Model variable	Symbol	Std of error
Dry bulb temperature	T_{dry}	0.25
Wet bulb temperature	T_{wet}	0.5
Pressure difference betwen inside and outside of the duct	Δp	1
Dynamic pressure of the fluid	p_{d}	2.5
Atmospheric pressure	p_{atm}	1000

3.2 Calculated variables

The mass flow and the specific heat capacity in equation (26) are calculated with observable variables represented in Section 3.1. The moisture content of the air, ω, is needed in the calculation of mass flow and specific heat capacity. The moisture content of the air is also used in the calculation of other material properties than specific heat capacity. Material properties are then used in the calculation of the total heat transfer coefficient. For this reason the calculation of the mass flow and moisture content are presented in more details in this section.

3.2.1 Mass flow

The mass flow of air in equations (26) and (45) is the mass flow of dry air because it is independent of condensation. To calculate the mass flow of dry air the density of moist air is needed. It can be solved by the ideal gas law

$$p_{\mathrm{s}}V = nRT_{\mathrm{K}}, \tag{49}$$

where

V	is the volume of the gas	[m^3],
n	is the number of moles of gas	[mol],
R	is the ideal gas constant	[J/Kmol],
T_{K}	is the temperature in Kelvins	[K].

If we substitute $V = m/\rho$ and $n = m/M$ in equation (49) and solve the density from it, we will obtain

$$\rho_{\mathrm{ma}} = \frac{p_{\mathrm{s}}M_{\mathrm{ma}}}{RT_{\mathrm{K}}}, \tag{50}$$

where ρ_{ma} is the density of the moist air and M_{ma} is the molar mass of the moist air.

Molar mass M_{ma} of moist air can be solved from the equation

$$\frac{1}{M_{\mathrm{ma}}} = \frac{x_{\mathrm{da}}}{M_{\mathrm{da}}} + \frac{x_{\mathrm{wv}}}{M_{\mathrm{wv}}}, \tag{51}$$

where

x_{da}	is the mass fraction of the dry air	[-],
x_{wv}	is the mass fraction of the water vapour	[-],
M_{da}	is the molar mass of the dry air	[kg/mol],
M_{wv}	is the molar mass of the water vapour	[kg/mol].

Mass fractions are solved as

$$x_{\mathrm{da}} = 1 - x_{\mathrm{wv}} = \frac{m_{\mathrm{da}}}{m_{\mathrm{da}} + m_{\mathrm{wv}}} = \frac{1}{1+\omega}, \tag{52}$$

where m_{da} is the mass of the dry air and m_{wv} is the mass of the water vapour.

The flow rate of the fluid is also needed in the calculation of the mass flow. The measurement of the fluid flow in a ventilation duct with a velocity area method using Pitot static tubes is given next. The reference for that is in [8]. The dynamic pressure is related to the flow rate according to the law of Bernoulli

$$p_{\mathrm{d}} = \frac{1}{2}\rho v^2. \tag{53}$$

The dynamic pressure is measured in several grid points in the ventilation duct which transports the fluid to heat exchanger and forward from it. From those measurements we can solve the flow rates

$$v_{\mathrm{duct_{ma}}} = \sqrt{\frac{2p_{\mathrm{d}}}{\rho_{\mathrm{ma}}}}, \tag{54}$$

where $v_{\mathrm{duct_{ma}}}$ is the velocity of the moist air in the ventilation duct.

The mean flow rate can be calculated by

$$\bar{v}_{\mathrm{duct_{ma}}} = \frac{1}{n}\sum_{i=1}^{n} v_{\mathrm{duct_{ma}}i}, \tag{55}$$

where $\bar{v}_{\mathrm{duct_{ma}}}$ is the mean velocity of the moist air in the ventilation duct and $v_{\mathrm{duct_{ma}}i}$ is the velocity of the moist air at point i in the ventilation duct.

The volume flow for the moist air can be calculated by

$$q_{V_{\mathrm{ma}}} = kA_{\mathrm{duct}}\bar{v}_{\mathrm{duct_{ma}}}, \tag{56}$$

where

$q_{V_{\mathrm{ma}}}$	is the volume flow of the moist air	[m^3/s],
k	is the correction factor for the flow rate	[-],
A_{duct}	is the area of the cross-section of the duct	[m^2].

The factor k takes into account the number of the measurement points for the dynamic pressure in the duct and the geometry of the duct. In this thesis the value one was used for the factor k.

We obtain the mass flow $q_{m_{\mathrm{ma}}}$ of the moist air by

$$q_{m_{\mathrm{ma}}} = q_{V_{\mathrm{ma}}} \rho_{\mathrm{ma}}. \tag{57}$$

Finally the mass flow of the dry air, which is used in the model, is obtained from the mass flow of the moist air by

$$q_{m_{\mathrm{da}}} = \frac{q_{m_{\mathrm{ma}}}}{1+\omega}, \tag{58}$$

where $q_{m_{\mathrm{da}}}$ is the mass flow of the dry air.

At this point it is good to note that the velocity of the fluid in the duct in equation (55) is not usually the same as the velocity of the fluid in the heat exchanger in equation (9). The volume flow in the heat exchanger is, however, the same as in the ventilation duct. Thus the velocity in the heat exchanger can be solved from

$$v_{\mathrm{he}} A_{\mathrm{slots}} = \bar{v}_{\mathrm{duct_{ma}}} A_{\mathrm{duct}}, \tag{59}$$

where v_{he} is the velocity of the fluid in the heat exchanger and A_{slots} is the frontal surface area.

3.2.2 Moisture content of the air

The absolute water content or moisture content ω is a function of static pressure and dry and wet bulb temperature. Moist air is considered as a mixture of completely dry air and water vapour as an ideal gas mixture. Moisture content is given as a ratio of mass fractions of the water vapour and dry air (kg/kg here). It can be calculated as

$$\omega = \frac{m_{\mathrm{wv}}}{m_{\mathrm{da}}} = \frac{1.0048(T_{\mathrm{wet}} - T_{\mathrm{dry}}) + \omega_{\mathrm{cond}}(2501 - 2.3237 T_{\mathrm{wet}})}{2501 + 1.86 T_{\mathrm{dry}} - 4.19 T_{\mathrm{wet}}}. \tag{60}$$

The constants for the equation as well as the equations for the moist air in this section are taken from [10, p. 299] and the physics behind the equations is explained in [11, pp. 613,621].

The moisture content of saturated air can be calculated by the equation

$$\omega_{\mathrm{cond}} = 0.62197 \frac{p_{\mathrm{sat}}}{p_{\mathrm{s}} - p_{\mathrm{sat}}}, \tag{61}$$

where p_{sat} is the saturation pressure of water vapour.

The saturation pressure of the water vapour can be estimated, for instance, by the formula

$$p_{\mathrm{sat}} = \exp\left(11.78 \frac{T_{\mathrm{wet}} - 99.64}{T_{\mathrm{wet}} + 230}\right). \tag{62}$$

3.2.3 Material properties

The physical properties of fluids are called material properties. Here in the modelling of the heat exchanger we need specific heat capacity, thermal conductivity, dynamic viscosity and density. For water, the calculation of material properties is easier than for air. For moist air the dry air and the water vapour are handled separately and somehow combined after that. The water vapour content always affects the material properties of air. In the context of material properties the word "correlation" in the literature means the fitting of a material property to temperature, pressure and moisture content. There are several alternative correlations for material properties presented in literature. The density of the air was already presented in equation (50). The rest of the correlations for the material properties used here are presented in Appendix 1.

The temperature is changing inside the heat exchanger and the values of material properties are changing accordingly. The most proper way of taking this into account in the calculation of the overall heat transfer coefficient would be integrating the values for material properties through the whole heat exchanger. The arithmetic mean of the material properties at the inlet and the outlet is easier to calculate. However, temperatures at the inlets for the calculation of material properties inside the whole heat exchanger was used.

3.3 General form of a model

In general, a model can be written in the form

$$s = f(x, \theta), \tag{63}$$

where

s	is the vector of the state variables	[-],
f	is the model function	[-],
x	is the vector of the control variables	[-],
θ	is the vector of the unknown model parameters	[-],

$$y = g(s), \tag{64}$$

where y is the vector of observations and g is the observation function.

In the heat exchanger model without phase change the independent, measured or known, control variables are

$$x = (G_{\mathrm{he}}, G_{\mathrm{duct}}; T_{\mathrm{wet_h}}, T_{\mathrm{wet_c}}, p_{\mathrm{d_h}}, p_{\mathrm{d_c}}, T_{\mathrm{dry_h}}, T_{\mathrm{dry_c}}; \Delta p_{\mathrm{h}}, \Delta p_{\mathrm{c}}, p_{\mathrm{atm}})^{\mathrm{T}},$$

where the geometry variables G are the most controllable variables, but can be considered as constants once the geometry is fixed. That is actually done hereafter. The following six variables — the temperatures and the dynamic pressures — can be considered more controllable (active) variables than the last three (passive) control variables. This would be the case if we had laboratory circumstances. In paper mills, however, none of the variables are conrollable in that sense due to circumstances. Flow values, moisture contents and other process technical dimensioning variables are calculated based on the measured independent variables as described in the previous sections.

For the unknown parameters we choose

$$\theta = \begin{pmatrix} C \\ m \\ n_{\mathrm{h}} \\ n_{\mathrm{c}} \end{pmatrix},$$

the constants in equation (8). Note that all the other model parameters — the constants of the material property correlations, for instance — are treated as known and fixed values. Only the above parameters θ are used to calibrate the model against real measurements.

The state variables are

$$y = s = \begin{pmatrix} T_{\mathrm{h_o}} \\ T_{\mathrm{c_o}} \end{pmatrix}.$$

4 Inverse problems and the Bayesian inference

Parameter estimation and finding the confidence limits for parameters with given measurements is a typical example of an inversion problem. For a reference to inverse problems see [12]. By taking the measurement noise into account, we can write the general form of a model as

$$y = f(x, \theta) + \epsilon, \tag{65}$$

where ϵ is the noise vector or the error vector of observations.

Given the data y and x we should be capable of estimating the parameters θ by the Bayes formula, the probability distribution of the parameters:

$$\pi(\theta) = p(\theta|y) = \frac{p(y|\theta)p(\theta)}{p(y)} = \frac{p(y|\theta)p(\theta)}{\int p(y|\theta)p(\theta)\mathrm{d}\theta}, \tag{66}$$

where

$p(\theta\|y)$	is the posterior distribution (also the notation $\pi(\theta)$ is used)	[-],
$p(\theta)$	is the prior distribution	[-],
$p(y\|\theta)$	is the likelihood density function	[-],
$p(y)$	is the normalising factor	[-].

If we assume that noise in the model in equation (65) is independent and identically distributed (i.i.d.) Gaussian noise $\epsilon \sim N(0, \sigma^2 I)$, the likelihood function becomes

$$p(y|\theta) = Ce^{-\frac{1}{2\sigma^2}SS}, \tag{67}$$

where C is a constant, σ^2 is the error variance and where the SS-function

$$SS = \sum_{\mathrm{i}=1}^{\mathrm{n}} \left(y_{\mathrm{i}} - f(x_{\mathrm{i}}, \theta)\right)^2 = ||y - f(x, \theta)||_2^2 \tag{68}$$

includes the model as a squared sum of the residuals.

Integrating the normalising factor in the denominator, even numerically, is often a difficult task. In the next section we discuss the Metropolis–Hastings algorithm — a practical way

of solving the posterior distribution without a need for integration.

4.1 The Metropolis–Hastings algorithm

The Markov Chain Monte Carlo method (MCMC) is a process which combines the Markovian property to the Monte Carlo method. The Markovian property means that the next point in the random process only depends on the previous one and no other points. The Monte Carlo methods refer to random sampling.

The Metropolis–Hastings algorithm (MH) is MCMC-method which can numerically solve the posterior distribution in the Bayes formula. It is an algorithm, where a move towards a better parameter estimate is always accepted, as in any optimisation method. But unlike in optimisation methods usually, a step towards a worse direction is also accepted with some probability.[2] The Metropolis–Hastings algorithm is represented in Algorithm 1. For reference see [13, p. 270].

Algorithm 1 The Metropolis–Hastings algorithm

1. Set $i = 1$ and choose a starting point θ_{i}
2. Generate the candidate θ^* from the proposal distribution $q(\theta^*|\theta_{\mathrm{i}})$
3. Choose
$$\theta_{\mathrm{i}+1} = \begin{cases} \theta^* & \text{with probability} \quad \alpha(\theta_{\mathrm{i}}, \theta^*), \\ \theta_{\mathrm{i}} & \text{with probability} \quad 1 - \alpha(\theta_{\mathrm{i}}, \theta^*), \end{cases}$$
where
$$\alpha(\theta_{\mathrm{i}}, \theta^*) = \min\left\{1, \frac{p(\theta^*|y)}{p(\theta_{\mathrm{i}}|y)}\right\} \overset{\text{MH}}{=}^{3} \min\left\{1, \frac{p(\theta^*|y)q(\theta_{\mathrm{i}}|\theta^*)}{p(\theta_{\mathrm{i}}|y)q(\theta^*|\theta_{\mathrm{i}})}\right\} \tag{69}$$
4. Set $i = i + 1$ and go to 2

A good starting point for the algorithm, the maximum likelihood estimate $\hat{\theta}$, is achieved, for example, by minimising the sum of the squares of the residuals in the model. We set $i = 1$ and $\theta_1 = \hat{\theta}$ and set θ_1 as the first value in the chain. Then we choose a new candidate θ^* from the proposal distribution, usually centred at θ_{i}, thus near it. In step three

[2] In simulating annealing, for example, a step towards worse direction is also accepted but the probability of accepting bad movements is decreasing, approaching zero during the optimisation.

[3] The version were the proposal distribution is symmetric is called the Metropolis algorithm. Hastings included an asymmetric proposal distribution. We assume a symmetric proposal hereafter.

we compare the posterior value of the new candidate and the posterior value of the last accepted value in the chain. If we are going upwards, we accept the candidate and add it as the last value to the chain. If we are going downwards (the candidate is worse than the last value in the chain), then we choose $u \sim \mathrm{U}(0,1)$ from the uniform distribution and accept θ^* if $u \leq \alpha(\theta_{\mathrm{i}}, \theta^*)$. If θ^* is accepted, it is added as the last value to the chain. Otherwise θ_{i} is added as the last value $\theta_{\mathrm{i}+1}$ to the chain. Then we go back to step 2 and repeat the algorithm until the chain is long enough. It can be shown that if the MCMC run is properly done and the chain is long enough it converges to the posterior distribution given in equation (66). The statistical parameters for the posterior distribution can be calculated from the chain.

In the adaptive version of the Metropolis–Hastings (AM) the proposal distribution is adapted to the posterior distribution by the covariance matrix of the chain [14]. A new proposal closer to the rejected one can also be tried [15]. This is called delayed rejection. A combination of them is called DRAM [16] and the usage of the mentioned transformations can be found in [17] or [18].

4.2 Indirect method for MCMC

Because solving the model by the equation system (26) is quite slow, a new approach was tested to decrease the computation time. That is an indirect *two-step* method where the MCMC run is divided into two phases.

If we assume the additive Gaussian error model in equation (65), the variance scaled SS-function is calculated with the direct MCMC method by

$$SS(\theta) = \sum_{\mathrm{i}=1}^{\mathrm{n}} \left(\frac{y_{\mathrm{i}} - f(x_{\mathrm{i}}, \theta)}{\sigma} \right)^2, \tag{70}$$

where n is the number of observations and x_{i} refers to the ith measurement (independent) and y_{i} refers to the ith response or observation (dependent).

In the two-step method we use scalar "pseudo parameter" $\tilde{\theta}$. In fact it is a scalar variable of the model, which hides all the real parameters behind itself in the model. The two-step

method can be used if the model can be described by the formula

$$y = f(x, \tilde{\theta}) + \epsilon = f(x, \tilde{f}(\tilde{x}, \theta)) + \epsilon. \tag{71}$$

where $\tilde{f}$ is the partial model function and $\tilde{x}$ is the set of model variables.

The first step of indirect MCMC method is represented in Algorithm 2. First we take one observation or measurement. Then normal MCMC run is done with that observation to obtain the posterior distribution (=chain) for the pseudo parameter. We go through every observation to obtain the corresponding posterior distributions for the pseudo parameters.

Algorithm 2 The first step of the indirect MCMC method

FOR $i = 1$ TO n

Run MCMC at ith measurement by using variance scaled SS-function

$$SS_{\mathrm{i}}(\tilde{\theta}_{\mathrm{i}}) = \left(\frac{y_{\mathrm{i}} - f(x_{\mathrm{i}}, \tilde{\theta}_{\mathrm{i}})}{\sigma} \right)^2 \tag{72}$$

to obtain n chains for posterior distributions $p(\tilde{\theta}_{\mathrm{i}}|y_{\mathrm{i}})$.

END

Next we use the posterior distributions of pseudo parameters $\tilde{\theta}_{\mathrm{i}}$ produced in the previous step as a data for step two. How that is done, can be seen in Algorithm 3. Performing steps one and two should yield the same posterior distribution $p(\theta|y)$ as the direct method gives. The size of the sample from the posterior distribution (from chain) in step two needs to be large enough and the inner sum needs to be scaled by the size of the sample from the chain.

Algorithm 3 The second step of the indirect MCMC method

Run MCMC by using the variance scaled SS-function

$$SS(\theta) = \sum_{\mathrm{i}=1}^{\mathrm{n}} \left(\sum_{\mathrm{j}=1}^{\mathrm{m}} \left(\frac{\tilde{\theta}_{\mathrm{ij}} - \tilde{f}(\tilde{x}_{\mathrm{i}}, \theta)}{\sigma_{\mathrm{i}}} \right)^2 / \mathrm{m} \right), \tag{73}$$

where m is the size of the sample $\tilde{\theta}$ from the posterior distribution $p(\tilde{\theta}_{\mathrm{i}}|y_{\mathrm{i}})$ of step one and σ_{i} is the variance calculated from that distribution.

When implementing the SS-function in a computer the variances in equation (73) could be calculated by chain outside the SS-function because their values are independent of the parameter values and do not change. Scaling the size of the sample in the posterior distribution $p(\tilde{\theta}_{\mathrm{i}}|y_i)$ outside the SS-function does not make calculation any faster. Squaring the residuals leaves a central mixed term $-2\tilde{\theta}_{\mathrm{ij}}\tilde{f}(\tilde{x}_{\mathrm{i}},\theta)$, which cannot be calculated outside the SS-function.

This method should be faster than the direct method if the model requires the usage of a root solver, an ode solver or some slow numerical method and step two is only some algebraic equations. The chains in the first step of the indirect method can be much shorter than a chain in the direct method, because the chain is mixed better in a case of just one parameter. In the first step of indirect method the adaptation of the proposal distribution can be done in every step because the calculation of the covariance matrix is an easy task with just one parameter.

5 Tests for the two-step indirect method

The normal direct and the new indirect method with three fast and simple toy examples, one nonlinear and two linear cases, will be compared in the following sections. It is especially important to use the same data in the comparisons if the number of the observations or the sample size of the data is small. The only difference in the comparisons should then be caused by the random character of the MCMC method.

5.1 Case study 1: Linear plane

The first case is a linear regression model

$$y_{\mathrm{i}} = \beta_0 + \beta_1 x_{\mathrm{i}1} + \beta_2 x_{\mathrm{i}2} + \cdots + \beta_{\mathrm{n}} x_{\mathrm{in}} + \epsilon_{\mathrm{i}}, \tag{74}$$

where β stands for regression coefficient. Model can be written in a matrix form as

$$\begin{pmatrix} y_1 \\ y_2 \\ \vdots \\ y_{\mathrm{m}} \end{pmatrix} = \begin{pmatrix} 1 & x_{11} & x_{12} & \cdots & x_{1\mathrm{n}} \\ 1 & x_{21} & x_{22} & \cdots & x_{2\mathrm{n}} \\ \vdots & \vdots & \vdots & \ddots & \vdots \\ 1 & x_{\mathrm{m}1} & x_{\mathrm{m}2} & \cdots & x_{\mathrm{mn}} \end{pmatrix} \begin{pmatrix} \beta_0 \\ \beta_1 \\ \vdots \\ \beta_{\mathrm{n}} \end{pmatrix} + \begin{pmatrix} \epsilon_1 \\ \epsilon_2 \\ \vdots \\ \epsilon_{\mathrm{m}} \end{pmatrix}. \tag{75}$$

By using the pseudo parameter $\tilde{\theta}_{\mathrm{i}}$ the model becomes

$$y_{\mathrm{i}} = \tilde{\theta}_{\mathrm{i}} + \epsilon_{\mathrm{i}},\ \tilde{\theta}_{\mathrm{i}} = \beta_0 + \sum_{\mathrm{j}=1}^{\mathrm{n}} \beta_{\mathrm{j}} x_{\mathrm{ij}},\ \mathrm{i} = 1, \ldots, \mathrm{n}. \tag{76}$$

In the indirect MCMC runs the pseudo parameter $\tilde{\theta}_{\mathrm{i}}$ is sampled in every measurement x_{i} as in Algorithm 2 to obtain the posterior distributions for the responses y_{i}. There is no need for a second step, because we now have the posterior distributions for the responses. We can directly solve the overdetermined equation group, equation (75), by minimising the least squares or by solving the normal equations to obtain the posterior distributions for the real parameters θ (here β_{i}).

While synthesising the data, values $[(-1,-1)^{\mathrm{T}},(1,-1)^{\mathrm{T}},(-1,1)^{\mathrm{T}},(1,1)^{\mathrm{T}}]^{\mathrm{T}}$ for x and $[1,1,1]^{\mathrm{T}}$ for β were used. The four first elements in the first column of the error vector $\epsilon_1 \sim N(0,1^2)$ multiplied by the square root of the error variance $\sigma = 0.5^2$ was added to the exact solution of the model. The noise vector ϵ_1 is given in Table 4. The marginal distributions for the five direct runs versus the five indirect runs for the parameters β_{i} are shown in Figure 9, as well as the predictive distributions calculated at $x = [1,1]^{\mathrm{T}}$. It can be seen that the results of the direct and the indirect method cannot be distinguished.

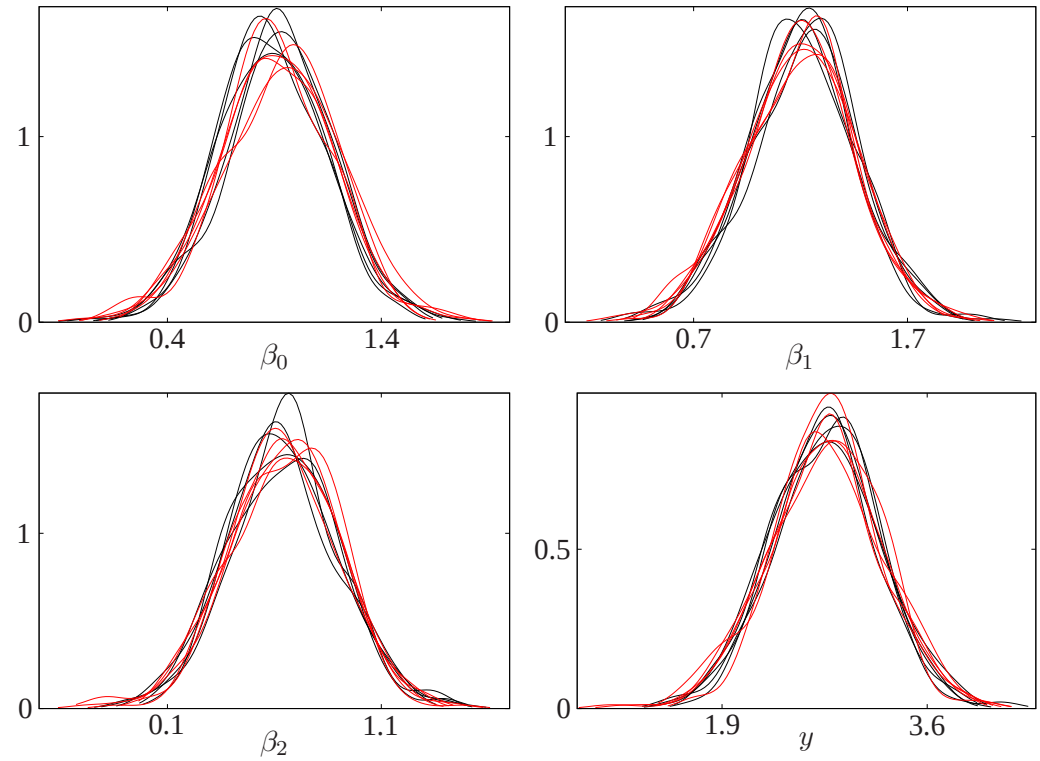

Figure 9: The marginal posterior distributions for the parameters β_{i} and the predictive distributions for the response y at $x = [1,1]^{\mathrm{T}}$. The red distributions are produced by the direct method and black distributions by the indirect method.

5.2 Case study 2: Slope of line

In the previous section we used only the first step of the indirect method. Next we will test the second step of the indirect method by using MCMC. The model for the second test case is

$$y_{\mathrm{i}} = \theta x_{\mathrm{i}} + \epsilon_{\mathrm{i}}, \tag{77}$$

where x and y are vectors of n points in the one dimensional space and θ is one scalar. Thus the MCMC run corresponds to fitting the data to a straight line passing the origo

and determining the posterior distribution for the slope. First y was calculated at $x = [50, 100, 150, 200]$ with $\theta = b = 1$. Then the data was generated by adding noise to the exact solution of the model from the first four elements of the noise vector $\epsilon_1 \sim N(0, 1^2)$ multiplied by the square root of the error variance $\sigma = 0.5^2$ as in case 1. In the first step four MCMC runs were done by going through the elements of x one by one. So basically the posterior distributions for the pseudo parameters $\tilde{\theta}_{\mathrm{i}} = b_{\mathrm{i}}$ (the slopes for the four lines) were estimated. In each run there where one measurement (the control variable and the corresponding response) and one parameter. The model in equation (77) was substituted in place of the model in equation (72). In the second step the posterior distributions of the slopes of all the lines were put together to produce a real model parameter $\theta = b$. As in the first step, the same model was used but now it was substituted in the place of the model in equation (73). Thus here $f = \tilde{f}$ in equation (71). The posterior distributions of the slope from the five normal MCMC runs and the five indirect MCMC runs produced by the two-step method are shown in Figure 10. There are some differences among the runs but the posterior distributions do not differ between the methods as it can be seen.

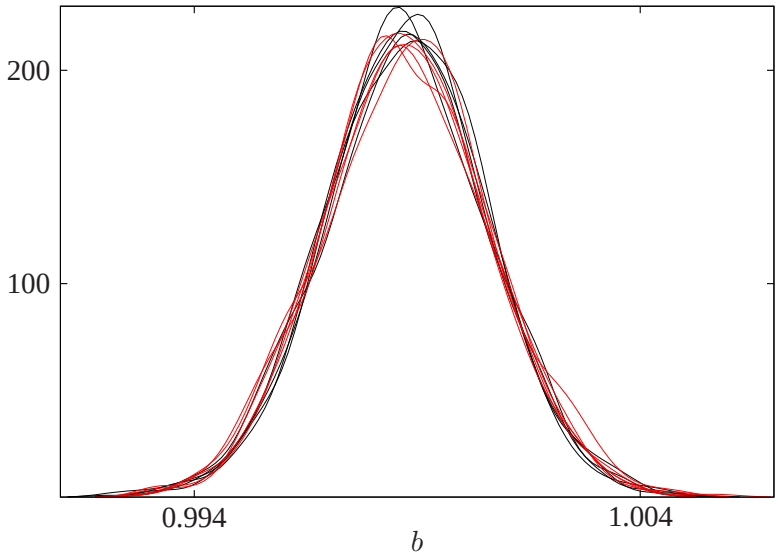

Figure 10: The marginal posterior distributions for the slope of the line. The red distributions are produced by the direct method and the black distributions by the indirect method.

5.3 Case study 3: Arrhenius law

The nonlinear test case was an analytical solution of the differential equation in reaction kinetics. The usage of the analytical solution is faster than the usage of the numerical solver and in that sense more ideal as a test case. The equation for the analytical solution

is

$$y = e^{-kt}, \tag{78}$$

where k is the rate constant of the reaction and t is the time.

The Arrhenius law states that the rate of the kinetic reaction depends on temperature in the following way

$$k = Ae^{\frac{-E}{RT_{\mathrm{K}}}}, \tag{79}$$

where

T_{K}	is the temperature in Kelvins	[K],
R	is the ideal gas constant	[J/Kmol],
A	is the pre-exponential factor in Arrhenius law	[mol/dm^{3}s],
E	is the activation energy in Arrhenius law	[J/mol].

There are plotted reaction curves for different temperatures in Figure 11(a). It can be seen that the amount of the substrate is decreasing when time is passing. The decreasing is faster with higher temperatures.

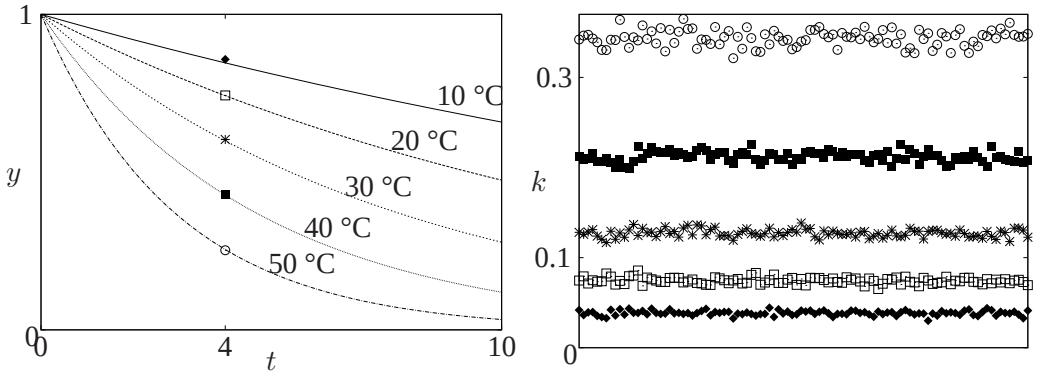

(a) Reaction kinetics at different temperatures.

(b) Samples from MCMC chains

Figure 11: Data for the first step (a) and for the second step (b) of the indirect method in case 3.

Synthetic data was generated at five different temperatures, $T_{\mathrm{C}} = [10, 20, 30, 40, 50]^{\mathrm{T}}$°C, by using parameter values $A = 10^6$ and $E = 4 \cdot 10^4$. The first five elements from the error vector $\epsilon_1 \sim N(0, 1^2)$ of Table 4 multiplied by the square root of the error variance level $\sigma^2 = 0.01^2$ were added to the exact solution of the model. Only one measurement for each temperature was done (dots in figure $\Rightarrow n = 5$). The substrate consentration y_{i} was measured at the temperature T_{i} when four time units had passed from the beginning of the

process. In this nonlinear case the pseudo parameter is $\tilde{\theta} = k$, the real model parameter is $\theta = [A, E]^{\mathrm{T}}$, control variables are $x = [t, T]^{\mathrm{T}}$ and $\tilde{x} = T$. In the first step five separate MCMC runs were done by sampling k_{i} at corresponding temperatures T_{i} so that equation (78) is substituted in the place of the model in equation (72). The samples from the chains for different temperatures are shown in Figure 11(b).

After that the chains $\tilde{\theta}_{\mathrm{i}}$ from the first step were used as data for the second step. There equation (79) gives the model in equation (73). The predictive distribution for the central temperature $T_{\mathrm{C}} = 30$°Cwas calculated. The comparisons of the direct and the indirect two-step methods are plotted in Figure 12. Again, we see that the results agree with both methods.

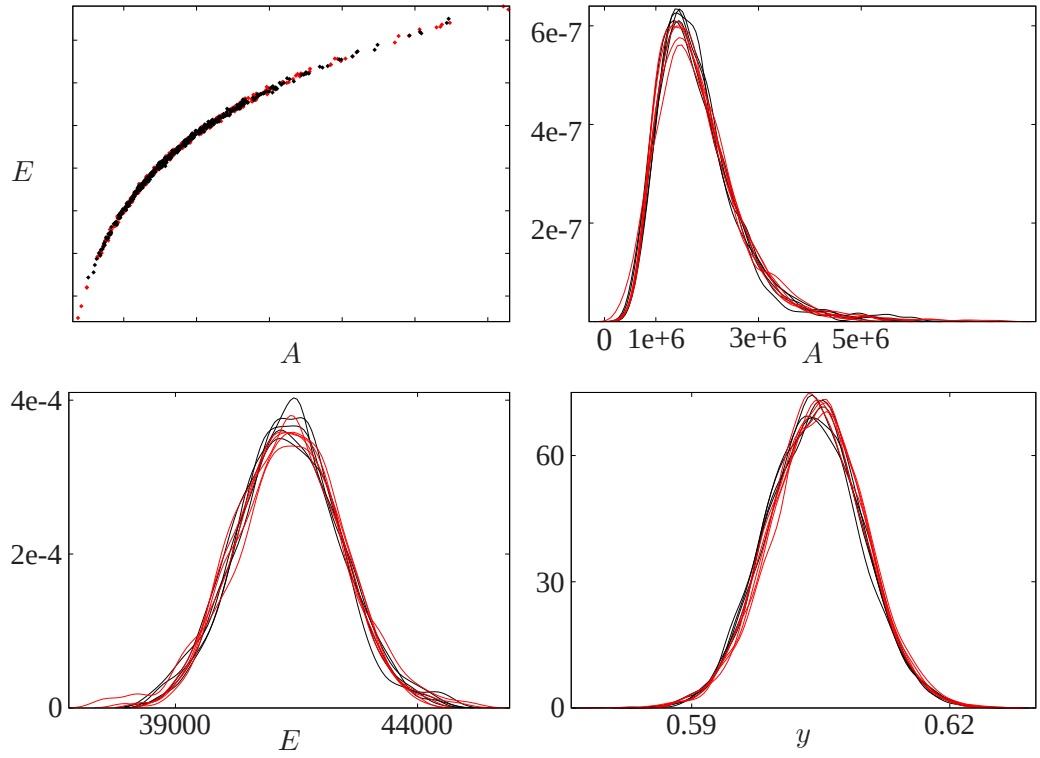

Figure 12: The posterior distribution and the marginal posterior distributions for parameters A and E in the Arrhenius law. The distribution for the response y is calculated at $T_{\mathrm{C}} = 30$°C. The red distributions are produced by the direct method and the black distributions by the indirect method.

6 Statistical analysis of the heat exchanger model without phase change

The model given by the equation (26) was implemented by the Octave software so that all code could also be run in MATLAB. Some parts of the model were also implemented as Octave binary files by C++ to improve the performance of the code. The root founding routine `fsolve` was used to solve the model. The Octave `fsolve` cannot pass parameters to a model like the MATLAB `fsolve` can. Global variables were used for passing the values of parameters. The values of the parameters were saved to global variables before a call to `fsolve` and they were read from the global variables in the model. The DRAM toolbox [19] was used for MCMC runs.

In the heat exchanger model without phase change the parameter vector θ is given by equation (8), so that $\theta_1 = C$, $\theta_2 = m$, $\theta_3 = n_{\mathrm{h}}$ and $\theta_4 = n_{\mathrm{c}}$, where n_{h} and n_{c} are the powers of the Prandtl number for the hot and the cold side, respectively.

The predictive distributions represented here are obtained by solving the model with a sample from the posterior distribution of the parameters. In what follows, the black colour denotes distributions produced by the indirect two-step method and the red colour denotes distributions produced by the traditional MCMC method.

6.1 Comparison of the direct and indirect methods

There are 6 or 7 measured control variables in the model, depending on whether the atmospheric pressure is considered controllable or not. The rest are the dry bulb temperatures, wet bulb temperatures and dynamic pressures for both the hot and the cold side. Thus the total factorial design of the two level per control variable would yield at least $2^6 + 1$ measurements, 65 altogether, if the central point was included. For practical reasons this is too much. The measurements can be taken in different circumstances, so that the control variables are different, but still not necessary desirable. The number of measurements should be minimised because there is no online measuring and the circumstances for making the measurements are quite demanding and thus the measuring is expensive. There are no laboratories available for testing heat exchangers either. Considering all this, the data for a heat exchanger was generated by using eight measurements from the full factorial design and the central point, even though in practice it might be impossible to completely

manage the control variables.

The dynamic pressures $p_{\mathrm{d_h}}$ and $p_{\mathrm{d_c}}$ and the hot incoming dry bulb temperature $T_{\mathrm{dry_h}}$ had all possible two level combinations. The rest of the variables were combined but not with all possible combinations. Atmospheric pressure is not considered as a control variable here. The range for the control variables was nearly the same as the one typically used in the process technical dimensioning of heat exchangers. The measurement points for the control variables are given in Table 3 starting from the second column and ending in the seventh column. The value for the atmospheric pressure was 101325 Pascals and zero Pascals for the pressure difference between the inside and the outside of the ventilation duct in the hot and the cold side for every measurement.

Table 3: Measurement points. Columns 2-7 are values of the control variables. The moisture content ω and ρv are process technical dimensioning variables according to which the factorisation is done.

	Control variables						Dimensioning variables			
Sample	$T_{\mathrm{dry_h}}$	$T_{\mathrm{dry_c}}$	$T_{\mathrm{wet_h}}$	$T_{\mathrm{wet_c}}$	$p_{\mathrm{d_h}}$	$p_{\mathrm{d_c}}$	ω_{h}	ω_{c}	ρv_{h}	ρv_{c}
1	82.0	31.5	42.6	23.4	69.7	81.6	0.039	0.015	11.0	12.1
2	79.0	35.0	45.1	25.7	58.0	56.1	0.050	0.017	10.1	10.0
3	79.0	35.0	40.2	21.1	81.4	56.1	0.033	0.010	12.0	10.0
4	79.0	28.0	40.2	25.7	58.0	107.2	0.033	0.020	10.1	14.0
5	79.0	28.0	45.1	21.1	81.4	107.2	0.050	0.013	11.9	14.0
6	85.0	28.0	45.1	21.1	58.0	56.1	0.047	0.013	10.0	10.1
7	85.0	28.0	40.2	25.7	81.4	56.1	0.030	0.020	11.9	10.1
8	85.0	35.0	40.2	21.1	58.0	107.2	0.030	0.010	10.0	13.9
9	85.0	35.0	45.1	25.7	81.4	107.2	0.047	0.017	11.9	13.8

The values for the wet bulb temperatures were calculated backwards from the moisture contents when the dry bulb temperatures were known. Actually, the moisture content is used as a process technical dimensioning variable instead of the wet bulb temperature. At the hot side the moisture content ω was varying from 0.03 kg/kg to 0.05 kg/kg and in the cold side from 0.01 kg/kg to 0.02 kg/kg. For the hot side this is less than in the literature [10, p. 302] but it was used here to ensure that the heat exchanger was not going to condensate. After that the dynamic pressures were similarly calculated backwards from ρv_{he}, the multiplication of density and flow rate in heat exchanger. ρv_{he} is a process technical dimensioning variable rather than a dynamic pressure. The values for the process technical dimensioning variables ω and ρv_{he} used in the measurements as well as the mass flows are given in Table 3.

The data was made synthetically by adding noise from the normal distribution to the results of the model as in equations (65) and (71). First the model was solved in nine measuring points, thus exact values for the heat rate Φ and the outlet temperatures $T_{\mathrm{h_o}}$ and $T_{\mathrm{c_o}}$were obtained. Then data was generated by adding noise from the noise vector $\epsilon_1 \sim N(0,1)$ to $T_{\mathrm{h_o}}$ and from the noise vector $\epsilon_2 \sim N(0,1)$ to $T_{\mathrm{c_o}}$ multiplied by the error std level $\sigma = 0.25$. The error vectors for generating the synthetic data are given in Table 4. It was confirmed that the indirect method worked with other noise vectors, too.

Table 4: Exact results of the heat exchanger model at the measurement points of the control variables from Table 3. Noise vectors ϵ_1 and ϵ_2 and the corresponding synthetic data y generated by multiplying the noise vectors by the standard deviation of the error $\sigma = 0.25$ and adding the result to the outlet temperatures. Dew point of the hot side and the temperature marginal, marg $= T_{\mathrm{surf}} - T_{\mathrm{dew}}$, before condensation starts. Convective and overall heat transfer coefficients.

Sample	Φ	$T_{\mathrm{h_o}}$	$T_{\mathrm{c_o}}$	ϵ_1	ϵ_2	y_1	y_2	T_{dew}	marg	α_{h}	α_{c}	U
1	343	72.6	47.9	−0.1	−0.7	72.6	47.7	36.2	15.6	48	47	23.9
2	264	71.1	50.3	1.2	−0.3	71.4	50.2	40.3	11.8	45	41	21.4
3	279	71.9	51.2	−1.1	0.8	71.7	51.4	33.0	18.3	51	41	22.7
4	356	68.3	42.7	−0.7	−1.1	68.1	42.4	33.0	16.9	45	53	24.3
5	382	69.4	43.8	1.0	1.1	69.6	44.1	40.3	8.6	52	53	26.1
6	342	74.7	47.6	0.5	0.2	74.8	47.7	39.4	10.8	45	41	21.4
7	363	75.7	48.7	−0.6	2.0	75.6	49.2	31.6	17.6	51	41	22.7
8	346	74.5	49.5	−0.7	−1.1	74.3	49.2	31.6	24.8	45	53	24.1
9	373	75.5	50.6	−0.2	−0.6	75.5	50.4	39.4	16.1	52	53	26.1

For the heat exchanger model the "pseudo" parameter is $\tilde{\theta}_{\mathrm{i}} = U_i$ and the real model parameters are $\theta = [C, m, n_{\mathrm{h}}, n_{\mathrm{c}}]$ from equation (8) of the Nusselt number. The measured control variables are $\tilde{x} = x = [T_{\mathrm{dry_h}}, T_{\mathrm{dry_c}}, p_{\mathrm{atm}}, \Delta p_{\mathrm{h}}, \Delta p_{\mathrm{c}}, T_{\mathrm{wet_h}}, T_{\mathrm{wet_c}}, p_{\mathrm{d_h}}, p_{\mathrm{d_c}}]^{\mathrm{T}}$.

The pairwise comparisons of the parameters in the posterior distribution for the normal direct MCMC method and the indirect two-step method are shown in Figure 13. It is difficult to see the possible differences from that figure. For that reason the marginal distributions for the parameters from the three normal direct MCMC runs and the nine indirect two-step runs are plotted in Figure 14. In Figure 15 there are plotted predictive marginal distributions for responses in the central sample point number one in Table 3. There does not seem to be remarkable differences in the methods. For that reason the indirect two-step method have been used hereafter with the heat exchanger models. The indirect two-step method sped up the computation compared to the traditional direct method.

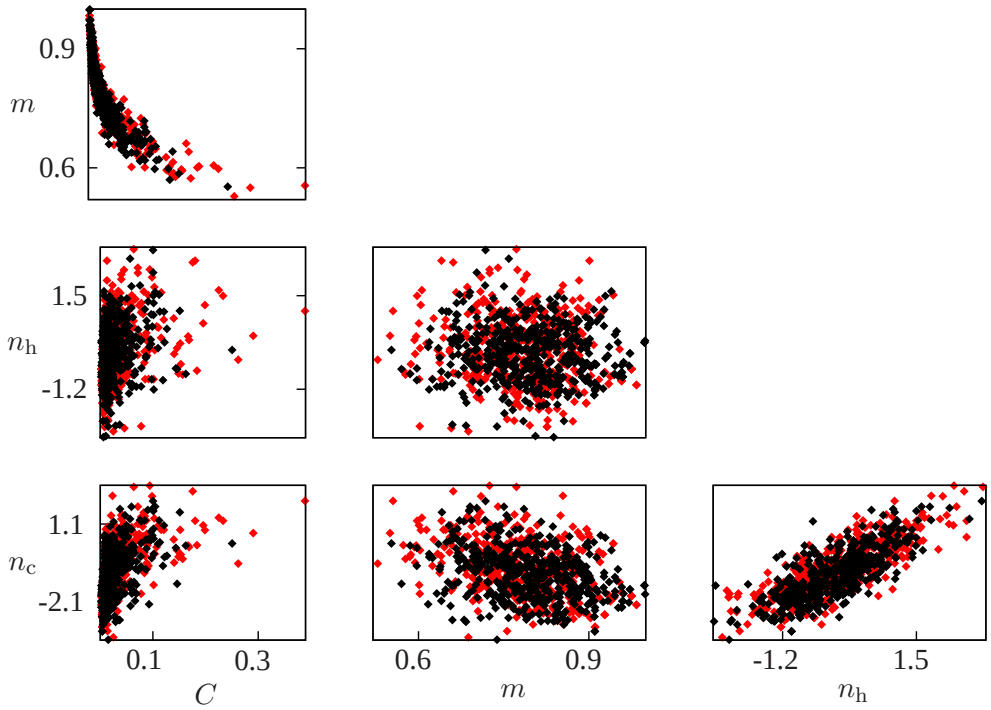

Figure 13: Pairwise comparisons of the heat exchanger parameters. The red distributions are produced by the direct method and the black distributions by the indirect method.

6.2 Effect of measurement sample size, design of experiments and error variance

Measurement sample size has an effect on the identifiability of the parameters. There has to be at least as many measurements as there are parameters in the model if we want the parameters to be identified at all. Here it means that we should have at least five measurements. Random effects can have a large effect on the results if the data is sampled only in few points. The smaller the size of the sample is the larger the probability that measurements of individual samples are differ from each other.

The more measurements there are the better the parameters should be identified. That can be seen in Figure 16. There are distributions for nine sample points given in Table 3 and distributions for full factorial design of the 65 sample points described in Section 6.1.There were no remarkable difference on the statistical parameters of the error vectors between 65 and nine sample points. The variances of the parameters in the posterior distribution are smaller for 65 sample points than for nine sample points. Therefore the distributions in Figure 16 are better identified for 65 sample points. This can be expected by the SS-function residuals: the sums of the residuals for large samples are larger than for small samples while the error variance remains the same. Then the likelihood of

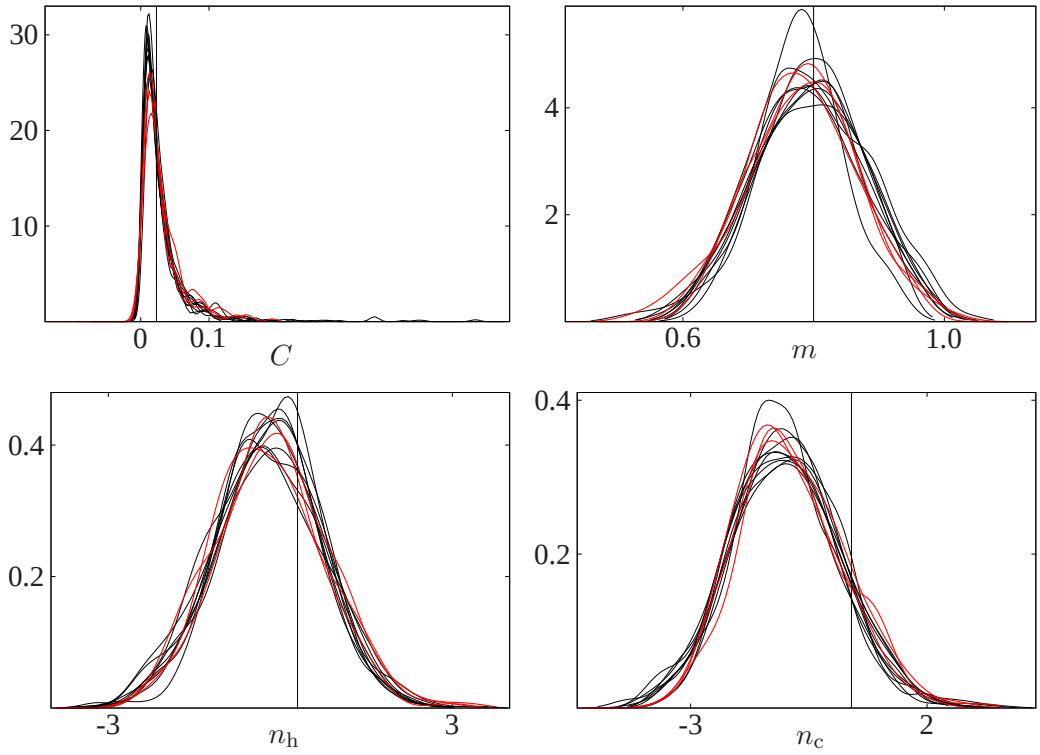

Figure 14: Marginal posterior distributions for the heat exchanger parameters. The red distributions are produced by the direct method and the black distributions by the indirect method. Vertical lines stand for literature values.

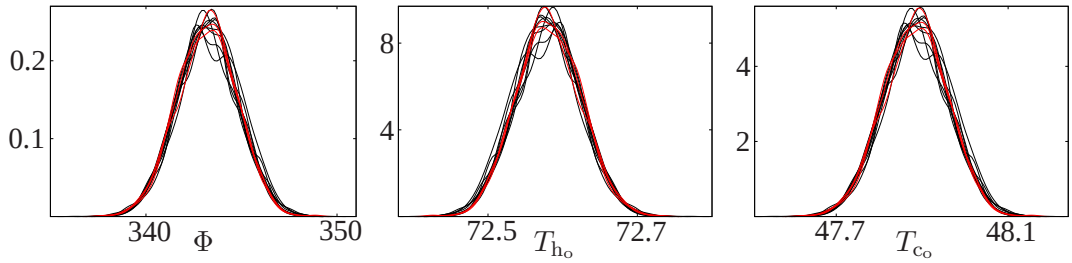

Figure 15: Distributions for the responses at sample point one from Table 3. The red distributions are produced by the direct method and the black distributions by the indirect method.

being accepted with the same value of parameters becomes smaller for larger sample sizes in equation (67).

Nine sample points will be used in thesis hereafter mostly for reasons described in section 6.1 but also for technical reasons[4]. Once the number of samples is fixed, the identifiability can be increased only by choosing more optimal samples. Choosing the sample size and the places of measurements is called design of experiments. In general, full or fractional

[4]The calculation of distributions with the faster indirect method for 65 sample points in Figure 16 took eight hours while the calculation of distribution for nine sample points took approximately one hour.

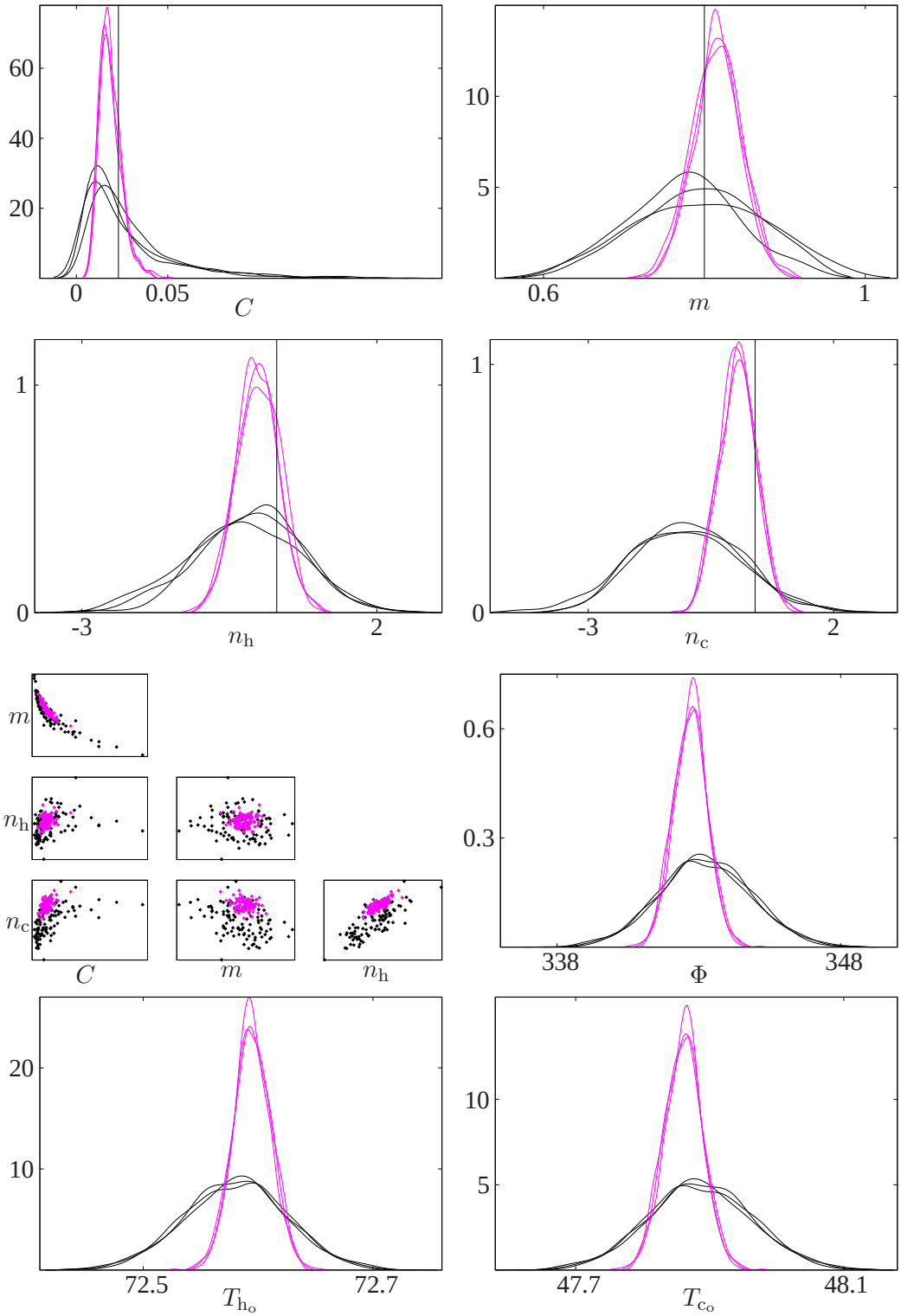

Figure 16: Posterior distributions for parameters and corresponding distributions for response. The black distributions are generated with nine sample points and the magenta distributions with 65 sample points. Vertical lines stand for literature values.

factorial design is better for identifying the parameters than randomly chosen points. Using D-optimality criteria or optimising the place of the sample points using the identifi-

ability of the posterior distribution directly as an objective function could possibly yield to even better identifiability of the parameters. The latter method was actually tested here by the evolutionary algorithm. Indeed, the identifiability measure (the sum of standard deviations of parameters) was decreasing. However, the identifiability of the parameters in the sample points generated by that method were not studied more strictly.

Here the error variance of the outlet temperatures was assumed to be $\sigma^2 = 0.25^2$ including both the errors in thermometer (small) and the circumstances (large). If the error variance of the outlet temperatures is assumed to be caused by the thermometer alone, the reasonable error variance might be $\sigma^2 = 0.025^2$. The comparison of the posterior distributions of parameters and predictive distributions can be seen in Figure 17. The data is generated by the error variance levels $\sigma^2 = 0.25^2$ and $\sigma^2 = 0.025^2$ using the same error vectors. It can be seen that for a smaller error variance the identifiability of the parameters is clearly better than for a larger error variance.

The values for the four constants in the Dittus–Boelter correlation are $C = 0.023$, $m = 0.8$, $n_\mathrm{h} = 0.3$ and $n_\mathrm{c} = 0.4$ in literature. The same values were used here in the generation of the data. The median values calculated for the parameters from the posterior distribution were different from those. The reason for that can be the skew distribution due to the small size of the sample. The values were, however, inside the two sided 95 % confidence or credibility intervals of marginal distributions as can be seen in Table 5. There are medians and two sided 95 % credibility intervals of marginal distributions for the parameters and the corresponding predictive distributions at the first sample point of Table 3 with a large error variance and a small error variance. There are also given limits and medians with a large error variance so that the error vectors ϵ_1 and ϵ_2 in Table 4 were interchanged and the order of the elements was reversed when the data was synthesised.

The widths of the predictive distributions for hot outlet temperatures were approximately half of the widths for cold outlet temperatures. Ratio for standard deviations of predictive temperature distributions in hot outlet and in cold outlet in the central design point was 1.7 for all cases described above. However, ratios for standard deviations of the noise in the synthetic hot and cold outlet data did not remain the same among cases.

It can be seen that the range for constant m, the power of Reynolds number, was much more than the range for constant n, the power of Prandtl number. It is expected because the Prandtl number for air was only a little less than one (≈ 0.7) with used dimensioning while the values for the Reynold's number were thousands. If water has been used as a fluid, constant n would not probability has been varying so much because the Prandtl

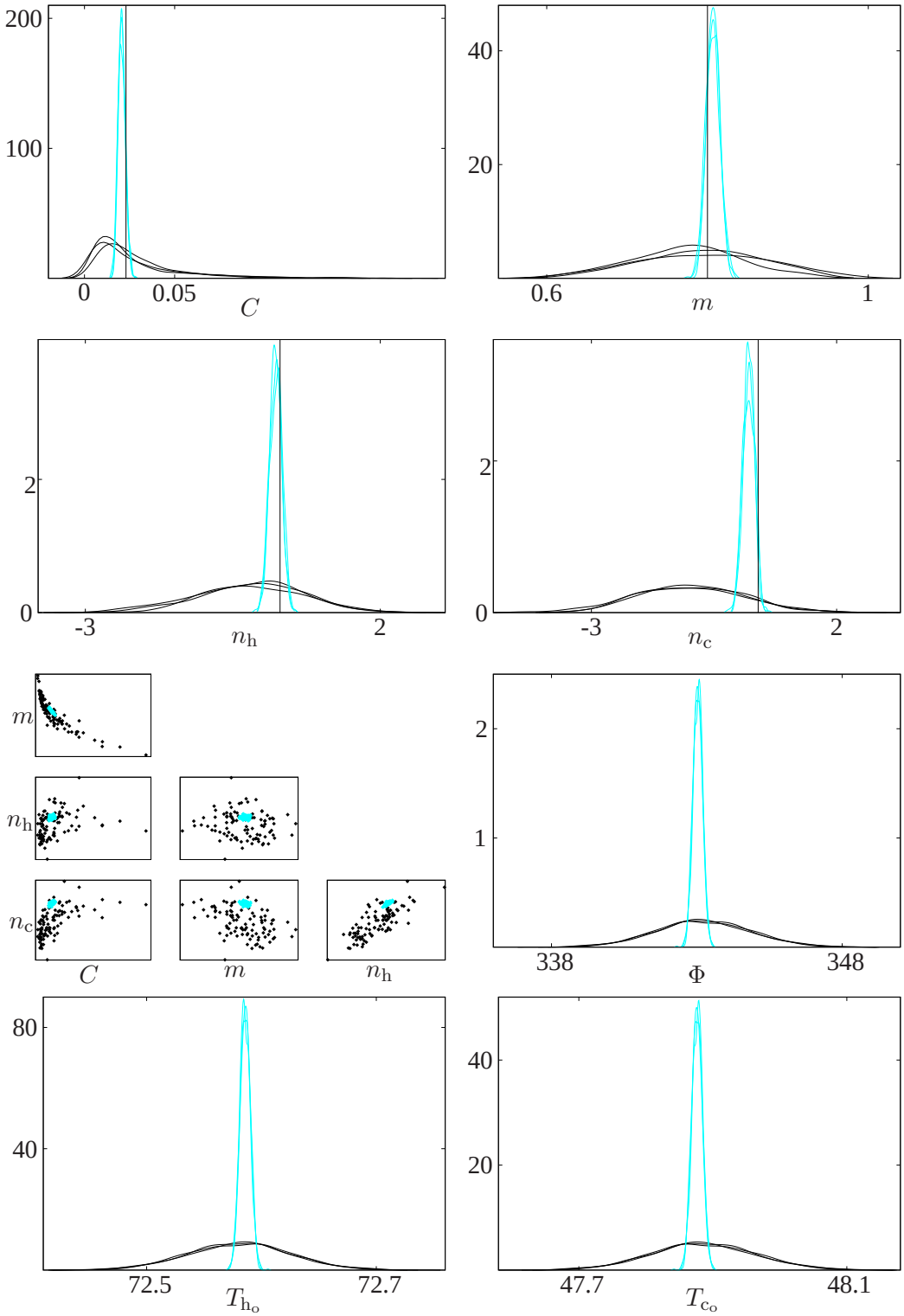

Figure 17: Posterior distribution for parameters and marginal distributions for prediction. The black distributions are generated with error level $\sigma^2 = 0.25$ and the cyan distributions with error level $\sigma^2 = 0.025$. Vertical lines stand for literature values.

number for water is approximately 10.

Table 5: Credibility intervals and medians of posterior distributions for parameters C, m, n_{h} and n_{c} in the Dittus–Boelter correlation and the corresponding predictive distributions at the first point in Table 3. The values given in the literature (the first column) were used in the synthetisation of the data. $\theta_{0.025}$ and $\theta_{0.975}$ are the 2.5 % and 97.5 % fractiles, respectively. The median is $\theta_{0.5}$. The error variance in the large noise column is $\sigma^2 = 0.25^2$. The error variance in the small noise column is one tenth of that. The reverse noise uses the same error vectors as large noise but the error vectors were interchanged and reversed.

		Large noise			Small noise			Reverse noise		
θ	Literature	$\theta_{0.025}$	$\theta_{0.5}$	$\theta_{0.975}$	$\theta_{0.025}$	$\theta_{0.5}$	$\theta_{0.975}$	$\theta_{0.025}$	$\theta_{0.5}$	$\theta_{0.975}$
C	0.023	0.003	0.019	0.110	0.017	0.021	0.025	0.012	0.068	0.360
m	0.8	0.63	0.79	0.95	0.79	0.81	0.82	0.57	0.72	0.87
n_{h}	0.3	−2.1	−0.2	1.6	0.0	0.2	0.4	−2.5	0.4	2.8
n_{c}	0.4	−3.1	−1.0	1.3	0.0	0.2	0.4	−0.3	2.0	4.3
y	Literature	$y_{0.025}$	$y_{0.5}$	$y_{0.975}$	$y_{0.025}$	$y_{0.5}$	$y_{0.975}$	$y_{0.025}$	$y_{0.5}$	$y_{0.975}$
Φ	343	338	343	349	342	343	344	338	342	348
$T_{\mathrm{h_o}}$	72.6	72.4	72.6	72.7	72.6	72.6	72.6	72.5	72.6	72.7
$T_{\mathrm{c_o}}$	47.9	47.6	47.9	48.1	47.8	47.9	47.9	47.6	47.8	48.1

6.3 Usability of the same posterior distribution among different geometries of the heat exchanger

Is it possible to change the geometry of the heat exchanger and to calculate predictive distribution by using the chain of parameter values produced with another geometry? The need for that might emerge, for example, in the optimisation of the geometry if predictive distributions were used [20, pp. 49-67]. Using the same chain in different geometries would be much faster compared to running MCMC inside the optimiser for each geometry separately. Three geometries were created for testing: A, B and C. The design of experiments was the same for all geometries and is given in Table 3. Geometries are described in Table 6. Here all marginal distributions generated with geometry A are drawn with a solid line, all marginal distributions generated with geometry B are drawn with a dotted line and all marginal distributions generated with geometry C are drawn with a dashed line.

In the first test case geometries A and B were used. The heat surface areas were different but not the frontal surface areas. Thus the flow rate in the heat exchanger and the overall heat transfer coefficient U did not change. An MCMC run with the geometry A was made and the posterior distribution got from that is denoted hereafter as chain A. Similarly, the

Table 6: Heat exchanger geometries A, B and C for test cases. U, the overall heat transfer coefficient, and A, the surface area, are the same for the whole geometry. The rest of the dimensions are given for both the hot and the cold sides separately. The lengths are meters and the areas are square meters.

Geometry	A		B		C	
Surface area A	388		487.5		742.5	
U for 1. sample point	23.9		23.9		15.3	
Side	Hot	Cold	Hot	Cold	Hot	Cold
Cross-sectional area	3.16	1.69	3.16	1.69	6	2.48
Duct area	3	1.5	3	1.5	3	1.5
Height of the plate	2	1	2.5	1.25	3	1.25
Width of the slot	0.016	0.017	0.016	0.017	0.02	0.02
Number of slots	98	97	79	78	100	99
Hydraulic diameter	0.032	0.034	0.032	0.034	0.040	0.039

posterior distribution produced with the geometry B is denoted hereafter as chain B. The predictive distributions for geometry A was calculated by using chain A and B separately. Then the predictive distributions for geometry B were calculated by using chain B and A, separately as before. The predictive distributions did not differ as can be seen in Figure 18.

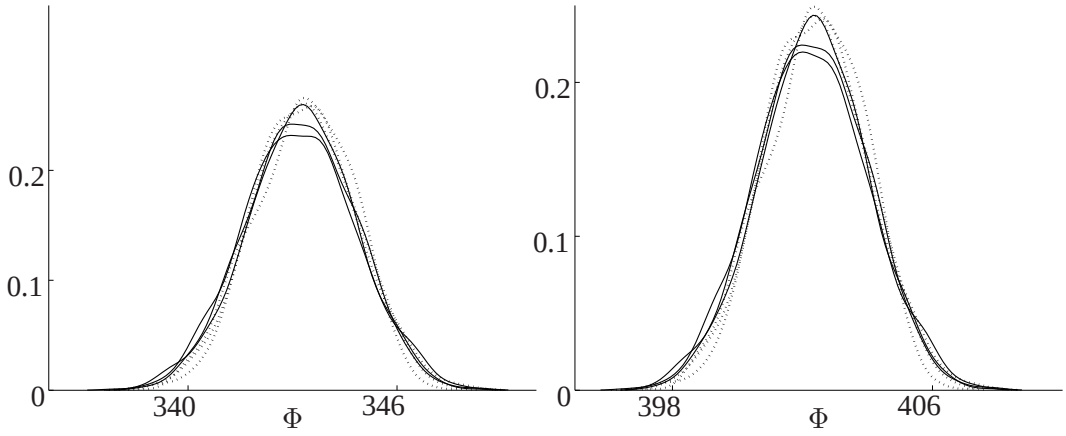

Figure 18: Marginal distributions for the responses. The solid line is generated with chain A and the dotted line is with chain B. The figure on the left is for geometry A and the figure on the right for geometry B.

In the second test case also the frontal surface areas were different ($\Rightarrow$ different U). The predictive distributions were calculated as described before but now for geometries A and C. There are differences between the predictive distributions in Figure 19. The predictive distributions have a larger standard deviation when generated with a wrong chain compared to one generated with a correct one.

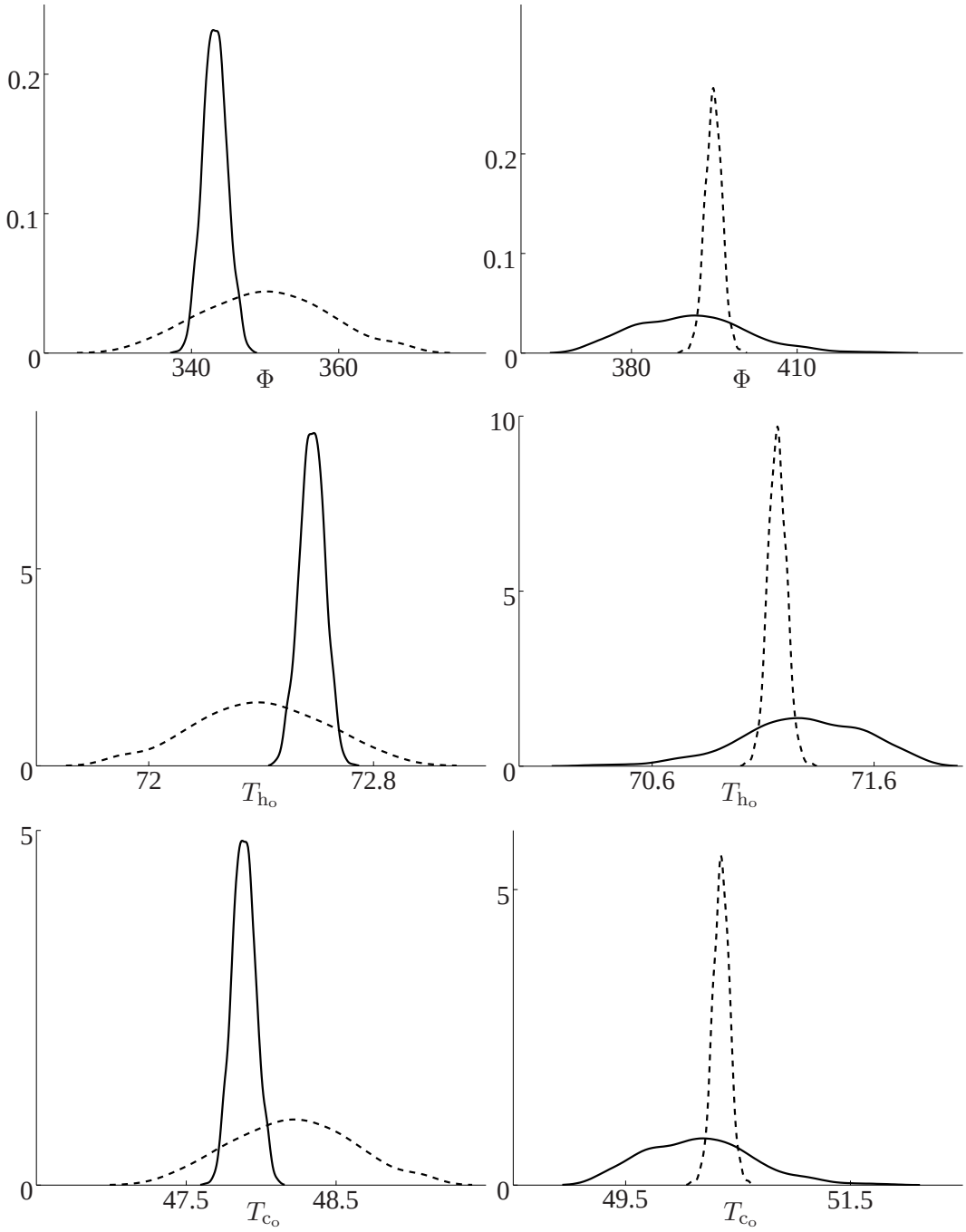

Figure 19: Marginal posterior distributions for the responses. The solid line is generated with chain A and the dashed line with chain C. Figures on the left hand side are for geometry A and figures on the right hand side for geometry C.

6.4 Error in measured variables

In this section an error in the control variables x is assumed so that they are not considered strictly given as usually. Actually all the measurements have an error, also the control variables x. It has been assumed that the measurement error is Gaussian and there

is no systematic error. Thus the mean of the measurement error is zero and the strict measurement is the mean of the distribution of the measurements.

In an MCMC run the measurement distribution of the control variables can be taken into account by including the x variables to a parameter vector in addition to real parameters. Those extra parameters are called *error-in-x* parameters here. Then we give a prior variance σ_x^2 and a prior mean μ_x from the normal distribution to the x parameters. The prior μ_x for an error-in-x parameter is the value of the corresponding strict control variable x. The prior σ_x^2 for an error-in-x parameter is the variance of the estimated error in the value of the corresponding control variable x. In the MCMC run the value for the control variable x is picked from the corresponding error-in-x parameter instead of using the strict control variable x in the calculation of the model in the SS-function. How the Metropolis–Hastings algorithm takes the priors into account, can bee seen, for example, in [17, p. 17].

If we assume that there is an error in the measurement of the control variable, we should get wider distributions for the model parameters compared to the case where we assume a strict control variable x. This was tested with the linear test case, see equation (77). The error variance of x ($\sigma_x^2 = 2^2$) was set to be sixteen times the error variance of y ($\sigma_y^2 = 0.5^2$). It can be seen in Figure 20 that the distribution is broader in the unstrict case compared to the strict case.

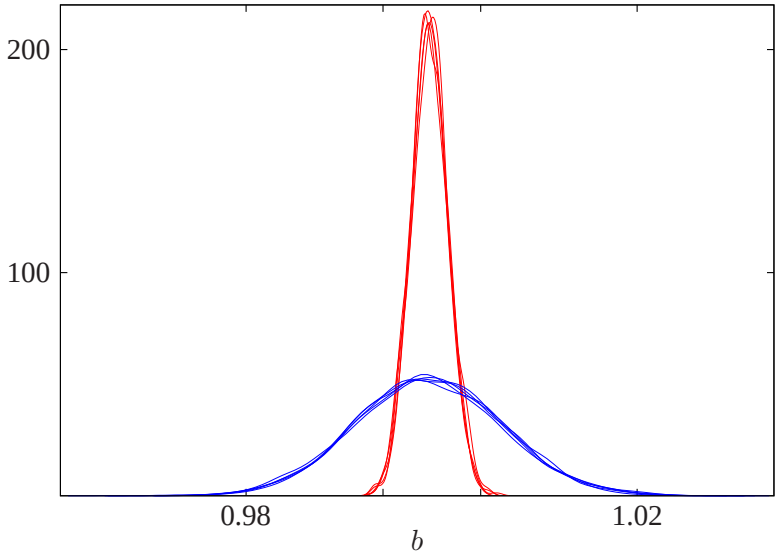

Figure 20: Comparison of the posterior distributions of the slopes for strict and error-in-x case in linear test case 2. The red distributions are generated assuming a strict measurement. The blue distributions are generated assuming an error in the measurement of the x variable. All distributions are produced by the direct method.

For nonlinear Arrhenius case in equation (78) the error variance $\sigma_T^2 = 1$°C in the measurement of the temperature was used. The predictive distribution were generated by using only the real parameters of the chain. The error-in-x parameter was replaced by the strict, or the prior mean μ_T value of temperature in the calculation of the prediction. The predictive distributions were calculated at the central sample point. The unstrict predictive distributions for response at 30°C were wider as can be seen in Figure 21.

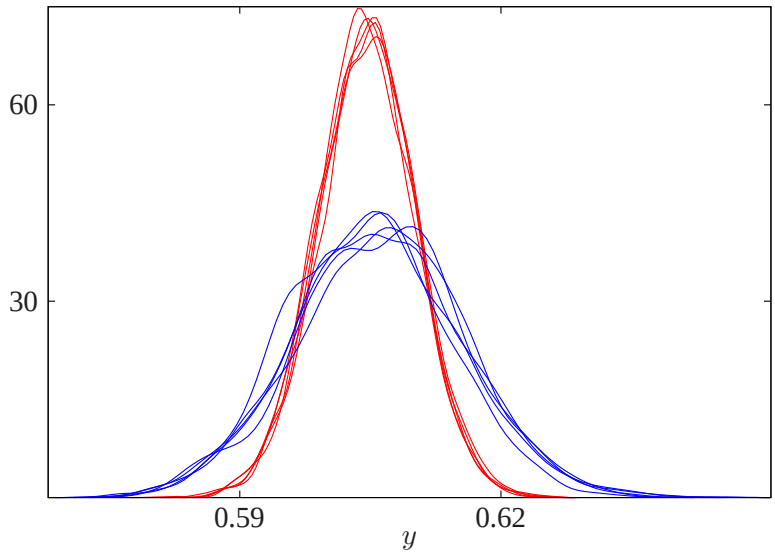

Figure 21: Marginal posterior distributions of responses in nonlinear test case (Arrhenius law) at 30 °C. The red distributions are produced by a chain where x was assumed to be a strict measurement. The blue distributions are produced by a chain where an error in the measurement of the x was assumed. All distributions are produced with the direct method.

Finally, an MCMC run with the heat exchanger model was done by using unstrict control variables. For simplicity, control variables were considered unstrict only in the second step of the indirect method. The same chains from the first step were used as data for making the comparison of the strict and error-in-x cases more reliable. The standard deviations described in Table 2 were squared to get the prior error variance σ_x^2 in the control variables and in the three measured but not controllable variables (p_{atm}, Δp_{h} and Δp_{c}). The values given in Table 3 were used for prior μ_x. For p_{atm} 101325 Pascals was used and for Δp_{h} and Δp_{c} zero Pascals were used as prior μ_x.

Every measurement of one control variable propagates one error-in-x parameter. Thus the use of the nine sample points given in Table 3 and all six control variables and the three measured but not controllable variables as error in x parameters propagated 81 error in x parameters in addition to the four real parameters, 85 parameters altogether. Even that is still a simplification. In reality the dynamic pressure is measured in several grid points as

described in Section 3.1.1. If we had had the grid of six measurement points on both the hot and the cold side, it would have led to 175 parameters altogether.

The predictive distributions were generated by using the model parameters only. Error-in-x parameters were replaced by the strict, or the prior mean μ_x values of the corresponding measured variables in the calculation of prediction. In Figure 22 there is a comparison of the predictive distributions generated with unstrict posterior distributions and with strict posterior distributions. The predictive distributions generated with unstrict posterior distributions are little wider than distributions generated with strict posterior distributions but the difference is not remarkable.

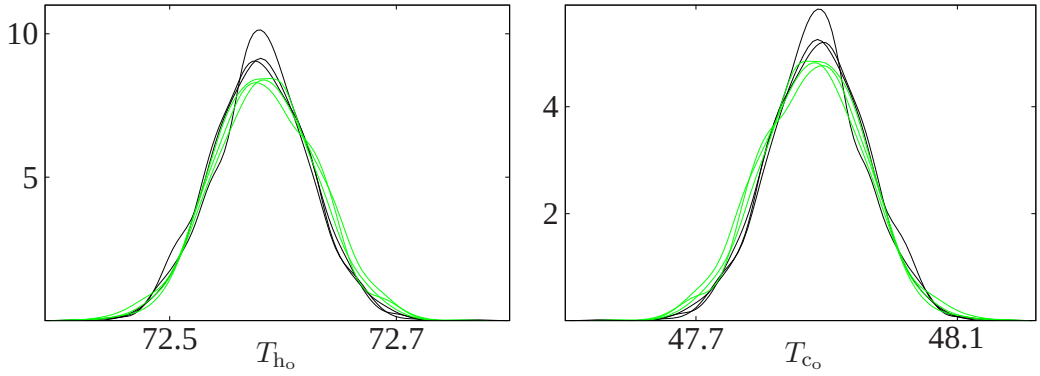

Figure 22: Marginal distributions for responses. The black distributions are produced by a chain where x was assumed to be a strict measurement. The green distributions are produced by a chain where there were assumed to be an error in the measurement of the x. Both chains were produced with the indirect method.

7 Numerics of the condensing surface model

The purpose here was to improve an earlier version of the condensing surface model. All material properties were treated as constants here unlike in the case of the heat exchanger model without phase change. Thus the convective heat transfer coefficients were also constants. On the cold side water is used as a fluid here in the examples. Moisture content of the hot air was 0.164 kg water vapour / 1 kg dry air and dew point temperature was 61°C. The values used in the example case are given in Table 7.

Table 7: Numerical values used in the condensing surface heat exchanger

Model variable	Air	Water
Inlet temperature [°C]	68	10
Mass flow [kg/s]	30	20
Convective heat transfer coefficient [W/m^{2}K]	45	6000

The model for the condensing heat exchanger described in Section 2.4 is a mechanical dimensioning problem model, which means that the heat surface area is not known but the incoming temperatures are known as well as the outgoing cold temperature. The model can be transformed by a numerical trick from a mechanical dimensioning problem model to a model where the area is known and the outgoing cold temperature is unknown. There is a connection between the cold outgoing temperature and the area in both directions. Changing from the mechanical dimensioning problem model to the case where a heat exchanger exists (and the area is known) becomes a root founding task in one dimension as can be seen in Figure 23. There the area A of the heat exchanger is plotted as a function of the cold output temperature $T_{\mathrm{c_o}}$.

Some nongradient based methods were tested, such as bisection, secant, regula falsi and the Muller method, to solve the root in Figure 23. In the Muller method [21, pp. 52-53] the value of the model is solved at three points (blue squares) and the parabola (blue line) in the figure is fitted to those points to estimate the function. The value of the function at the root of the parabola is calculated. That becomes the new point (red square) to fit the parabola when one point is dropped away in the next iteration of the algorithm. For the secant method a secant line is used instead of the parabola to estimate the function. The existing `fsolve`-solver could not be used because `fsolve` cannot be called inside `fsolve` at least in Octave.

The model cannot be solved if cold water should be heated too much. In that case the local incoming cold temperature inside the heat exchanger exceeds the local outgoing hot

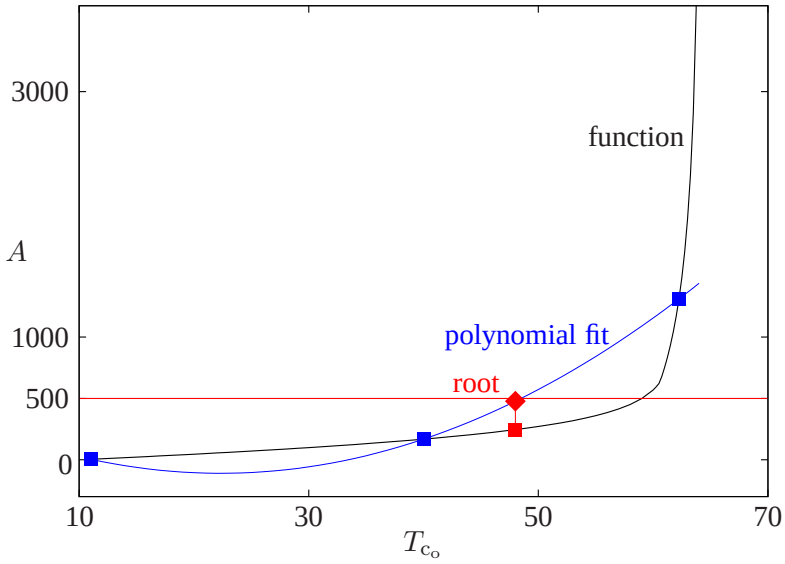

Figure 23: Root founding = converting a mechanical dimensioning problem model to an existing area model

temperature at the place where the heat exchanger starts to condensate in the calculation of the dry area in equation (13). Then the logarithmic mean temperature difference obtains an imaginary value. This problem did not occur if the cold fluid was air. How much the cold water can be heated depends on the circumstances. There are plotted areas versus cold outgoing temperatures with different hot incoming temperatures in Figure 24. It can be seen that the area needed to heat the cold fluid to a certain temperature starts to increase rapidly after the dew point. Above the dew point condensation does not happend, heat exchanger is less effective and more area is needed to achieve the desired temperature.

7.1 Effect of the initial guess

Function solver `fsolve` needs to get at least a function for root finding and starting point as parameters. When the constant values were used as initial guesses, or starting values for the function solver `fsolve` in the first cell, the solver could not converge to a correct solution in all circumstances. The solver does not necessarily converge even if the solution exists. Having the starting guess near the root leads to convergence more probably.

An “intelligent” adaptive method to estimate the initial guess for the differences in difference equation (45) was used. The basic idea is to estimate the solution for the whole heat exchanger and then divide the estimate by the number of the cells. For example, the

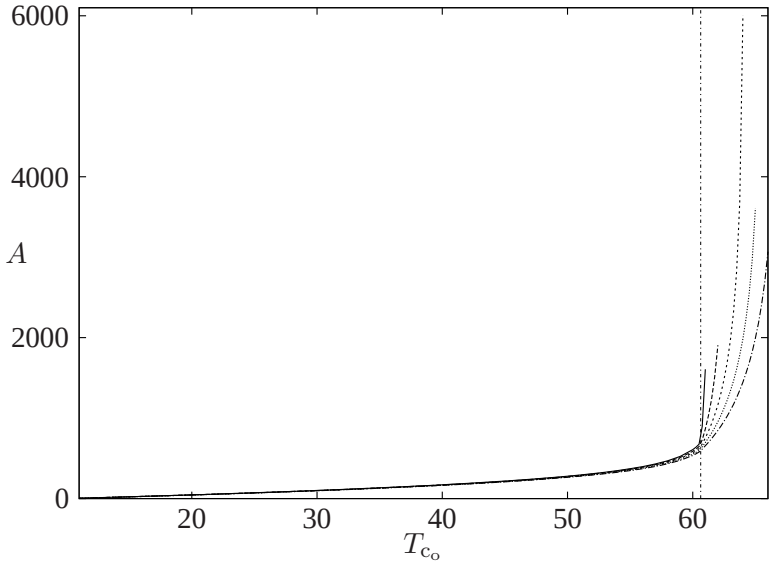

Figure 24: Area vs. cold outgoing temperature with different incoming hot temperatures. For the lower incoming temperatures the inflection is more rapid. The vertical line is the dew point.

difference of the heat rate on the cold side $\Delta\Phi_c$ in one cell can be calculated exactly by dividing the heat rate on the cold side $\Delta\Phi_c$ by the number of the cells. For the area this kind of estimation is impossible because actually we should solve the area but we cannot know it beforehand. But our initial guess for ΔA should, of course, be an estimate for the total area divided by the number of the cells. For the temperature difference of the condensate ΔT_{cond} the calculation of the estimate is more difficult. The initial value for the temperature of the condensate can be calculated by equation (44) but the outgoing value cannot be known. It should not drop below the temperature of the incoming cold fluid. Thus their difference divided by the number of the cells can be used as the initial guess. For the enthalpy difference Δh the heat rate on the cold side divided by the hot mass flow and that divided by the number of the cells gave a considerably good estimate everywhere. With the calculation of the initial guess for the difference in the moisture content $\Delta\omega$ the situation is somehow similar to the ΔT_{cond}because we know the incoming value for the moisture content but we do not know the outcoming value. If we also assume here that the outgoing hot temperature reaches the value for the incoming cold temperature, we can calculate the moisture content at that temperature, subtract it from the incoming one and divide the result with the number of the cells.

Once the first cell was solved, the solution obtained by difference equation (45) was used as an initial guess for cell two. Similarly, the solution of the previous cell was used as an initial guess in the next cell hereafter.

7.2 Retrial of the solution in the case of the fail of the convergence

Octave `fsolve` uses FORTRAN 77 MINPACK subroutine hybrd. It returns an info argument, which reveals the success of the convergence of the solution. The solver could not converge to the correct solution with initial starting guess when the outgoing cold temperature exceeded 60°C, which can be seen in Figure 25 as a drop in the function. It can also be seen, that the solver did not converge after a successful start in the following cells. The problem was solved by repeatedly starting the solver randomly near the initial guess or the solution from the previous step to get the correct function in Figure 25.

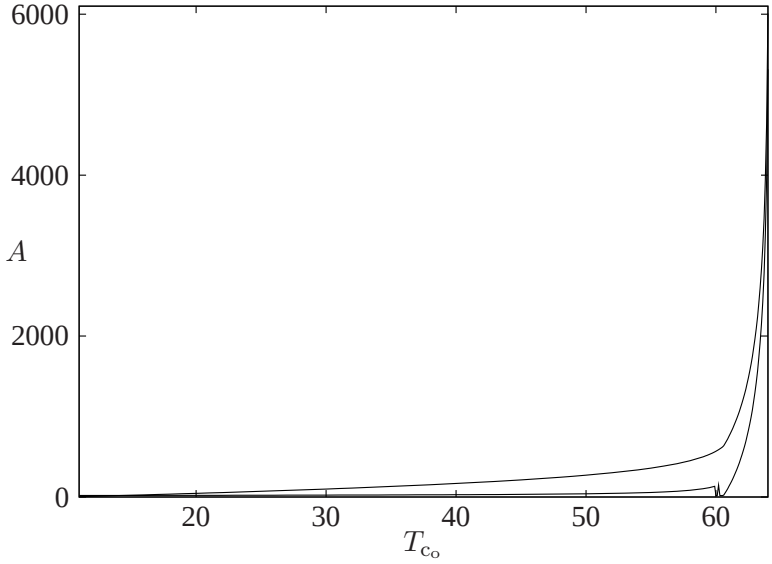

Figure 25: Failure to achieve a correct solution with a constant starting guess and one trial. In the upper solution an adaptive starting guess and a retrial of the solution are used.

7.3 Effect of the number of cells

A trade off exists between accuracy and time consumption. Both are increasing by the number of cells. The effect of the number of cells to the relative accuracy of the area at different outgoing temperatures is represented in Figure 26. The areas calculated with different cell numbers are compared to a case where the model is divided into thousand cells. That is considered “a true area” in the calculation of the percentage error and calculated areas for smaller cell numbers are considered. It can be seen that the absolute percentage error is increasing when the number of cells is decreasing.

With the low outgoing cold temperatures the number of cells does not remarkably affect the accuracy. The highest absolute percentage error is at the dew point.

Similar figures were produced with different incoming hot temperatures. The shapes of the error curves looked similar to the ones in Figure 26. By comparing the figures it was noticed that the nearer the incoming hot temperature was to the dew point the higher the percentage error of the area was.

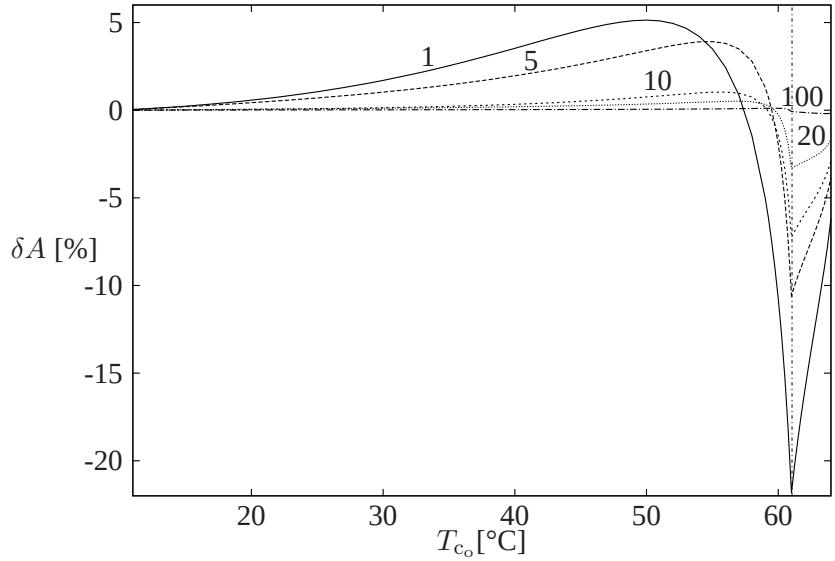

Figure 26: Effect of the number of cells to the relative accuracy of the area [%] at different outgoing temperatures T_{c_o} [°C]. Different lines are done with different cell numbers. The vertical line is the dew point.

8 Conclusions

The identification of parameters in the heat exchanger model without phase change was studied by MCMC methods. The Nusselt number, which is used in the calculation of the overall heat transfer coefficient, can be calculated by the Dittus–Boelter correlation, for example. The confidence limits for the constants (parameters) in the Dittus–Boelter correlation were found. There are combinations of parameter values bounded by the error so that especially the values for n — power of the Prandtl number — in the cold and the hot side can vary remarkably and even be negative. Naturally, nonphysical parameter values can be avoided using proper priors. The constant C can never be negative. It seemed that predicting the hot outlet temperature is less strict than predicting the cold outlet temperature.

The estimation of the right level of the error variance is crucial for the correct results when we use synthetic data. The pattern of the posterior distribution of the parameters can be affected by the level of the error variance only little but the width of the distributions can be chosen in advance. As we could see, we can get the results we want by choosing the correct level of the error variance when we make the data. That holds true also for the predictive distributions which can be used for the optimisation of heat exchanger networks. At least repeated pilot measurements should be taken for estimating the level of the error variance. Only real data can reveal the error caused by the model. As far as we are playing with synthetic data the results are only as good as our comprehension about the measurement error.

There is no convergence proof about the indirect two-step MCMC method. However, it seemed to work quite well here. The results did not differ compared to traditional method and it sped up the computation with the heat exchanger model. The performance analysis should be done in some other environment because part of the code, like the vectorised code, is executed in MATLAB and Octave as a compiled code while part of the code is still interpreted. When used with other models it might be good to compare the results of the indirect method to the traditional method. There is still a need for making the two-step method more automatic. The results of the second step depend on the data, which is a sample from the chains made in the first step. The results from the second step varied a little depending on how the sample was taken from chains of the first step. That should be studied more.

The new indirect method can be used, for example, in the design of experiments if we

try to maximise the identifiability of the MCMC chains. If a discrete sample space for measurements is used, we can run the first step in every sample point, save the chains and then combine these chains as needed in the second step. It is also possible to compute the first step in parallel. If it is possible to solve the model without the second step as in the first linear test case, it improves mixing of chains. We can produce one chain in every measurement point as in case one, because the chains in one dimensional parameter space are usually mixed better than in a multidimensional parameter space. Thus the multidimensional parameter space is changed to a one dimensional parameter space during the MCMC run and then back to the multidimensional parameter space to get the posterior distributions of the parameters by solving the model.

The use of same parameter posterior distribution with different geometries in the case of same process technical dimensioning is limited to geometries where heat exchangers have the same frontal surface areas. If we want to make other changes in the geometry when optimising the geometry using the posterior, we have to be more careful. It has to be taken into account that the predictive distributions produced with a wrong chain are wider than the distributions produced with a correct one and the means are not the same. The safest way is to produce an own chain for every geometry. The use of one chain in different geometries should be studied more.

It is not recommended to use error in the control variables in the same way as is done here if the measurement errors are below the described levels. Taking the error in the control variables into account is too demanding considering the benefit.

Our implementation of the condensing surface model could be used for the optimisation in [20]. In general, there is a need to find a pseudo parameter in condensing surface model, which hides all real parameters behind itself in order of the indirect method to be used. In the condensing surface model also the wet bulb temperature on the hot side has to be added to the measured response vector and respectively it has to be taken into account in the SS-function.

References

[1] Liikola, P. *Aineominaisuuksien mallinnustarkkuuden vaikutukset lämmönsiirtimien lämpöteknisessä simuloinnissa*. Master's thesis, Lappeenrannan teknillinen yliopisto, 2005.

[2] Incropera, F. P. and DeWitt, D. P. *Fundamentals of heat and mass transfer*. New York: Wiley, third edition, 1990. ISBN 0-471-51729-1, 919 pp.

[3] Lienhard IV, J. H. and Lienhard V, J. H. *A Heat Transfer Textbook*. Cambridge, Massachusetts: Phlogiston Press, third edition, [online: referred 21.7.2008], 749 pp. Available at: `http://web.mit.edu/lienhard/www/ahtt.html`

[4] VDI-GVC (ed.) *VDI Heat Atlas*. Düsseldorf: VDI-Verlag GmbH, first edition, 1993. ISBN 3-18-400915-7.

[5] Soininen, M. Dimensioning of Paper Machine Heat Recovery Recuperators. *Drying Technology*, 13(4):867–896, 1995. ISSN 0737-3937. doi:10.1080/07373939508916989.

[6] Heinonen, M. e-mail 13.05.2008. Finnish Centre for Metrology and Accreditation, Mikes.

[7] Riihimäki, K. Meetings and discussions. Balance Engineering, 2008-2009.

[8] Ilmatekniikan suunnitteluopas, osa 1. Turku: Valmet Oy ja Oy Mercantile AB, 1978.

[9] Rosti, A. Sääasema Nauvo, [online: referred 18.3.2009]. Available at: `http://arirosti.net/saa/`

[10] Karlsson, M. (ed.) *Papermaking Part 2, Drying*. Papermaking Science and Technology. Helsinki: Fapet Oy, 2000. ISBN 952-5216-09-8.

[11] Moran, M. J. and Shapiro, H. N. *Fundamentals of engineering thermodynamics*. Hoboken: John Wiley & Sons, Inc., fifth edition, 2004. ISBN 0-471-27471-2, 874 pp.

[12] Calvetti, D. and Somersalo, E. *Introduction to Bayesian Scientific Computing – Ten Lectures on Subjective Computing*, vol. 2 of *Surveys and Tutorials in the Applied Mathematical Sciences*. New York: Springer-Verlag, 2007. ISBN 978-0-387-73393-7, 202 pp.

[13] Robert, C. P. and Casella, G. *Monte Carlo statistical methods*. Springer texts in statistics. New York: Springer-Verlag, second edition, 2004. ISBN 0-387-21239-6, 645 pp.

[14] Haario, H., Saksman, E. and Tamminen, J. An adaptive Metropolis algorithm. *Bernoulli*, 7(2):223–242, 2001. doi:10.2307/3318737.

[15] Mira, A. On Metropolis-Hastings algorithm with delayed rejection. *Metron*, LIX(3-4):231–241, 2001.

[16] Haario, H., Laine, M., Mira, A. and Saksman, E. DRAM: Efficient adaptive MCMC. *Statistics and Computing*, 16(4):339–354, 2006. ISSN 1573-1375. doi:10.1007/s11222-006-9438-0.

[17] Laine, M. *Adaptive MCMC methods with applications in environmental and geophysical models*. Ph.D. thesis, Lappeenranta University of Technology, 2008.
Available at: `http://urn.fi/URN:ISBN:978-951-697-662-7`

[18] Solonen, A. *Monte Carlo Methods in Parameter Estimation of Nonlinear Models*. Master's thesis, Lappeenranta University of Technology, 2006.
Available at: `http://urn.fi/URN:NBN:fi-fe20071011`

[19] Laine, M. DRAM toolbox. 1.3.2007.
Available at: `http://www.helsinki.fi/~mjlaine/dram/`

[20] Habimana, D. *Statistical Optimum Design of Heat Exchangers*. Master's thesis, Lappeenranta University of Technology, 2009.
Available at: `http://urn.fi/URN:NBN:fi-fe200901141027`

[21] Gerald, C. F. and Wheatley, P. O. *Applied numerical analysis*. Addison-Wesley, 6th edition, 1999. ISBN 0-201-87072-X, 698 pp.

[22] Reid, R. C., Prausnitz, J. M. and Poling, B. E. *Properties of gases and liquids*. New York: McGraw-Hill, fourth edition, 1987. ISBN 0-07-051799-1, 741 pp.

[23] Goodfellow, H. and Tähti, E. (eds.) *Industrial Ventilation Design Guidebook*. San Diego: Academic Press, 2001. ISBN 0-12-289676-9, 1519 pp.

Appendix 1. Material properties used in this thesis

The following equations for material properties were used here. Liikola [1] collected them from the literature and used them in his Master's thesis

Thermal conductivity for dry air is obtained by

$$k_{\mathrm{da}} = 2.646\sqrt{T_{\mathrm{K}}}/\left(1 + \left(245.4 \cdot 10^{-12/T_{\mathrm{K}}}\right)/T_{\mathrm{K}}\right) \cdot 10^{-3}, \tag{1-1}$$

where k_{da} is the thermal conductivity of dry air [1, p.39] and T_{K} is the temperature in Kelvins. Thermal conductivity for water vapour is obtained by

$$k_{\mathrm{wv}} = \left(\frac{6.471\sqrt{T_{\mathrm{K}}}}{1 + \left(1737.3 \cdot 10^{-12/T_{\mathrm{K}}}\right)/T_{\mathrm{K}}} + 4.59 \cdot \left(10^{9.218 p_{\mathrm{bar}} \cdot (100/T_{\mathrm{K}})^4} - 1\right)\right) \cdot 10^{-3}, \tag{1-2}$$

where p_{bar} is the pressure in bars and k_{wv} is the thethermal conductivity of water vapour [1, p.39]. Value for the thermal conductivity of moist air is got by combining previous values by the method of Wilke

$$k_{\mathrm{ma}} = \frac{\tilde{x}_{\mathrm{da}} k_{\mathrm{da}}}{\tilde{x}_{\mathrm{da}} + \phi_{12}\tilde{x}_{\mathrm{wv}}} + \frac{\tilde{x}_{\mathrm{wv}} k_{\mathrm{wv}}}{\tilde{x}_{\mathrm{wv}} + \phi_{21}\tilde{x}_{\mathrm{da}}}, \tag{1-3}$$

where

k_{ma}	is the thermal conductivity of moist air	[W/mK],
$\tilde{x}_{\mathrm{da}}$	is the molar fraction of the dry air	[-],
$\tilde{x}_{\mathrm{wv}}$	is the molar fraction of the water vapour	[-],
ϕ	is the interaction term of the compounds	[-] [22, pp.407,410].

Value for interaction term is got from equation

$$\phi_{12} = \frac{\left(1 + \left(k_{\mathrm{da}}/k_{\mathrm{wv}}\right)^{1/2} \left(M_{\mathrm{wv}}/M_{\mathrm{da}}\right)^{1/4}\right)^2}{\left(8\left(1 + M_{\mathrm{da}}/M_{\mathrm{wv}}\right)\right)^{1/2}}. \tag{1-4}$$

Value for ϕ_{21} is got by interchanging the subscripts in the formula.

continues

Dynamic viscosity for dry air is got by equation

$$\mu_{\mathrm{da}} = \frac{1.458 \cdot 10^{-6}\sqrt{T_{\mathrm{K}}}}{1 + 110.4/T_{\mathrm{K}}} \tag{1-5}$$

where μ_{da} is the dynamic viscosity of the the dry air [1, p.39] and for water vapour by equation

$$\mu_{\mathrm{wv}} = (0.0361T_{\mathrm{K}} - 1.02) \cdot 10^{-6}, \tag{1-6}$$

where μ_{wv} is the dynamic viscosity of the the water vapour [1, p.39]. Value for the dynamic viscosity of moist air μ_{ma} is got by the method of Wilke as in previous case by substituting values for dynamic viscosity in place of values of thermal conductivity.

Specific heat capacity for dry air is got from formula

$$c_{p_{\mathrm{da}}} = 3.7348 \cdot 10^{-7}T_{\mathrm{C}}^2 + 1.8304 \cdot 10^{-5}T_{\mathrm{C}} + 1.0063, \tag{1-7}$$

where $c_{p_{\mathrm{da}}}$ is the specific heat capacity of dry air [1, p.40] and for water vapour from formula

$$c_{p_{\mathrm{wv}}} = \frac{32.24 + 1.924 \cdot 10^{-3}T_{\mathrm{K}} + 1.055 \cdot 10^{-5}T_{\mathrm{K}}^2 - 3.596 \cdot 10^{-9}T_{\mathrm{K}}^3}{1000 \cdot M_{\mathrm{wv}}}, \tag{1-8}$$

where $c_{p_{\mathrm{wv}}}$ is the specific heat capacity of water vapour [1, p.40]. Specific heat capacity for the mixture of dry air and water vapour is got by equation

$$c_{p_{\mathrm{ma}}} = c_{p_{\mathrm{da}}} + \omega c_{p_{\mathrm{wv}}}, \tag{1-9}$$

where $c_{p_{\mathrm{ma}}}$ is the specific heat capacity of moist air [23, p.81].